Distinct dissolved organic matter sources induce rapid transcriptional responses in co-existing populations of *Prochlorococcus*, *Pelagibacter* and the OM60 Clade

Adrian K. Sharma[1,6,7], Jamie W. Becker[2,6,7], Elizabeth A. Ottesen[1,3,6] Jessica A. Bryant[1,6], Solange Duhamel[2, 4,6] , David M. Karl[5,6], Otto X. Cordero[1], Daniel J. Repeta[2,6] and Edward F. DeLong[1,,6,*]

[1]Departments of Civil and Environmental Engineering and Biological Engineering, Massachusetts Institute of Technology, Cambridge, MA 02139

[2]Department of Marine Chemistry and Geochemistry, Woods Hole Oceanographic Institution, Woods Hole, MA 02543

[3]Department of Microbiology, University of Georgia, Athens, GA 30602

[4]Lamont Doherty Earth Observatory, Columbia University, Palisades, NY 10964

[5]Department of Oceanography, School of Ocean and Earth Science and Technology (SOEST), University of Hawaii, Honolulu, HI 96822

[6]Center for Microbial Oceanography: Research and Education (C-MORE), 1950 East-West Road, Honolulu, Hawaii 96822

[7]These authors contributed equally to this work

*To whom correspondence may be addressed. Email: delong@mit.edu

Manuscript intended for submission to Environmental Microbiology.

Abstract

A considerable fraction of the Earth's organic carbon exists in dissolved form in seawater. To investigate the roles of planktonic marine microbes in the biogeochemical cycling of this dissolved organic matter (DOM), we performed controlled seawater incubation experiments and followed the responses of an oligotrophic surface water microbial assemblage to perturbations with DOM derived from an axenic culture of *Prochlorococcus,* or high-molecular weight DOM concentrated from nearby surface waters. The rapid transcriptional responses of both *Prochlorococcus* and *Pelagibacter* populations suggested the utilization of organic nitrogen compounds common to both DOM treatments. Along with these responses, both populations demonstrated decreases in gene transcripts associated with nitrogen stress, including those involved in ammonium acquisition. In contrast, responses from low abundance organisms of the NOR5/OM60 gammaproteobacteria were observed later in the experiment, and included elevated levels of gene transcripts associated with polysaccharide uptake and oxidation. In total, these results suggest that numerically dominant oligotrophic microbes rapidly acquire nitrogen from commonly available organic sources, and also point to an important role for carbohydrates found within the DOM pool for sustaining the less abundant microorganisms in these oligotrophic systems.

Introduction

Nearly one half of global primary production occurs in the ocean (Field et al., 1998) where a diverse group of phytoplankton fix carbon and nutrients into particulate organic matter (Azam, 1998). Exudation of metabolic waste products, viral lysis and predation all release a portion of microbial production into the water column as dissolved organic matter (DOM), a complex mixture of biochemicals of varying biological availability (lability) (Carlson, 2002) that changes in time and space (Aluwihare et al., 1999; Kujawinski et al., 2009; Mopper et al., 2007). DOM supports secondary production and microbial respiration (Hansell et al., 2009; del Giorgio and Duarte, 2002), with heterotrophic and mixotrophic picoplankton representing the main consumers. Understanding how picoplankton interact with this dynamic DOM reservoir is complicated by the inherent phylogenetic and population diversity of microbial communities, the complexities of their collective metabolic properties and interactions, and by our ability to measure microbial assemblage activities and responses on appropriate temporal and spatial scales. For these reasons, characterizing and quantifying microbial DOM cycling in the sea is a significant challenge.

Several recent studies using experimental incubations of seawater or microcosm perturbations have explored the consumption of phytoplankton-derived isotopically labeled DOM sources by examining uptake patterns and changes in community composition among diverse taxonomic groups (Nelson and Carlson, 2012; Sarmento and Gasol, 2012). These studies indicate that organisms with different taxonomic affiliations and varying ecological growth strategies exhibit preferences in both the

phytoplankton-derived origin and compositional properties of DOM. Other recent studies have combined meta-omics approaches with temporal field observations or experimental microcosm perturbations in neritic systems to gain insight into taxon-specific microbial responses to changes in naturally derived sources of DOM (Poretsky et al., 2010; Rinta-Kanto et al., 2012; Teeling et al., 2012; Landa et al., 2013). These studies highlight patterns of taxon-specific resource partitioning of DOM, community strategies for energy scavenging under carbon limitation, and temporal successions of microbial populations in response to dynamic changes in natural DOM concentrations during a natural phytoplankton bloom. This previous work also demonstrates the utility of pairing DOM uptake experiments with meta-omics methodologies as a means of uncovering microbial taxa and metabolic strategies involved in marine DOM consumption.

The details of the functional and metabolic roles of specific microbial taxa in DOM degradation still remain largely unknown. Community response dynamics to DOM perturbations across short time scales are poorly understood, as most methods lack the necessary sensitivity to track transient responses. Such resolution would provide insight into the complex response mechanisms of microbial communities that result from both ecological variables and DOM resource partitioning. Here we report a microcosm-based DOM perturbation experiment in an oligotrophic region of the ocean focused on measuring rapid temporal response dynamics over a 36-hour period and the functional roles of oligotrophic taxa like *Prochlorococcus* and *Pelagibacter* that are ubiquitous in the open ocean (Lauro et al., 2009; Yooseph et al., 2010; Nelson and Carlson, 2012). Our

microcosm perturbations involved the addition of natural sources of DOM to seawater collected from within the surface mixed layer (35m) and placed in a temperature and light-controlled shipboard incubator. Incubations were conducted at Station ALOHA in the North Pacific Subtropical Gyre (NPSG), a region where the infrequency of deep-water mixing events results in low inorganic nutrient concentrations and limitation of primary production (Karl and Lukas, 1996; Karl et al., 2008). To study microbial communities under extreme oligotrophic conditions, perturbation experiments were conducted in late spring, a time of the year when the water column at Station ALOHA is highly stratified (Karl et al., 2012) and inorganic nutrient levels are frequently the most depleted (see supplementary figure S1).

To study differences in utilization of DOM from different sources, we examined the response of a single surface water microbial assemblage to perturbation with two distinct DOM types, comparing temporal observations from both treatments to a control microcosm. To examine breakdown of compounds in the standing DOM pool, we concentrated naturally occurring high-molecular weight dissolved organic matter (HMWDOM) on site from Station ALOHA surface seawater using an approach similar to that of McCarren *et al*. (2010). This size-fractionated DOM pool is considered to be "semi-labile", rich in polysaccharides (Aluwihare et al., 2005) and other high-molecular weight compounds that might be preferred by specialist copiotrophic taxa (McCarren et al., 2010). In order to examine breakdown of newly produced "labile" DOM, a second DOM source was prepared by concentrating the hydrophobic fraction of exudate from an axenic culture of *Prochlorococcus* strain MIT9313 (ProDOM). *Prochlorococcus* is the

dominant photoautotroph in nutrient poor ocean gyres and heterotrophic taxa in these regions are likely adapted to utilizing substrates derived from their photosynthate (Partensky et al., 1999; Bertlisson et al., 2005). The use of hydrophobic exudate material permitted direct chemical analysis of the treatment DOM by mass spectrometry, thus providing data on the nature of metabolites present and their size distribution.

We monitored microbial community responses to DOM amendments using a variety of methods and compared these observations to a control microcosm. Flow cytometry was used track cell growth over a 36-hour period and β-glucosidase exoenzyme activity was determined from selected time points to assess polysaccharide utilization. Both metagenomic and metatranscriptomic data were obtained before perturbation from the 35 m seawater used for our microcosm experiment, as well as at 36 h after amendment. Combined with metatranscriptomic data from the intervening 2, 12, and 27 h time points, this experiment generated a detailed look at short-term temporal and functional responses of different microbial taxa to changes in ambient DOM quantity and quality.

Results

Microbial community growth and exoenzyme activity

The HMWDOM amendment increased concentrations of both dissolved organic carbon (DOC) and dissolved organic nitrogen (DON) by approximately 140%, while the ProDOM amendment increased DOC and DON by only 7%. DOC concentrations with standard deviation (SD) derived from triplicate measurements were 191 μM C (SD 0.35)

for HMWDOM and 85.5 µM C (SD 0.35) for ProDOM, approximately 2.4x and 1.1x the ambient value of 79.9 µM C (SD 0.39) in the control microcosm. Both amendments increased DOC and DON concentrations in a manner that was proportional to the ratio of DOC:DON in the control. Despite these substantial differences in substrate quantity, both treatments induced similar patterns in growth relative to the control (Figure 1B and 1C), suggesting that the ProDOM treatment contained a higher proportion of labile DOM that could be converted into cellular biomass. Whereas the HMWDOM addition concentrated a fraction of the DOM already present in the sample, the ProDOM addition may have introduced exogenous DOM components to the community. Chemical analysis of the ProDOM material using high performance liquid chromatography-electrospray ionization mass spectrometry (HPLC-ESI-MS) revealed the presence of 1,491 low-molecular weight features with signal intensity at least 5-fold greater than the maximum noise level. These features ranged in size from 100.2-1,111.5 m/z, with the majority falling between 150-450 m/z. A control sample of Pro99 medium incubated without inoculation and processed as described above for the ProDOM amendment confirmed that these features were absent from the background medium.

Flow cytometric analysis indicated two stages of diauxic-like growth in the microbial community over the 36 h time course in both treatments relative to the control. The first and larger increase in cell numbers occurred between 12 and 19 h in both treatments relative to the control, where *Prochlorococcus* cells accounted for the majority of the total cell growth observed in treatments between these time points

(Figures 1B-1G). The second, less pronounced growth stage in both DOM amended microcosms occurred between 19 and 36 h. Here, *Prochlorococcus* comprised a much smaller fraction of the total cell growth in the HMWDOM and ProDOM microcosms, indicating that heterotrophic bacterioplankton could be responsible for the later increases in cell numbers.

The final time point in both treatments was characterized by an increase in β-glucosidase exoenzyme activity (Figure 1H and 1I) consistent with heterotophic growth at later time points. β-glucosidase is an enzyme produced by heterotrophic picoplankton that catalyzes the selective cleavage of glucosidic bonds in order to break down oligosaccharides into smaller sugars that can be transported into the cell. At the 36-hour time point, assays indicated a 130% increase in activity in the HMWDOM treatment and a 46% increase in activity in the ProDOM treatment relative to the control. These findings indicate the presence of polysaccharides in both treatments, and the level of β-glucosidase activity per unit carbon added in each treatment suggests that labile polysaccharides likely comprised a substantial proportion of the DOC in the ProDOM amendment. The observed increase in β-glucosidase activity at the final time point in both treatments was likely related to heterotropic growth and activity in the latter stages of the experiment.

Meta-genomic and -transcriptomic profiling of microcosm community structure

Table 1 outlines read numbers and database statistics for community DNA and cDNA samples sequenced from each of the different microcosms. Sequences derived from rRNA reads were identified *in-silico* and removed from all libraries, and taxonomic and functional annotations for the resulting non-rRNA reads were obtained from the top

BLASTX hit against the NCBI-nr database. The number of matches to a particular taxonomic group or NCBI-nr reference gene were normalized to the total number of reads with significant matches to the database, allowing for comparisons across samples.

Microbial community composition in the 35 m seawater used for our microcosm experiments (0 h DNA) was dominated by *Prochlorococcus* and *Pelagibacter* (Figure 2A). Surface ecotypes of *Prochlorococcus* (Johnson et al., 2006) comprised approximately 50% of metagenomic reads with a significant BLASTx hit to the NCBI-nr database The next most abundant group in our starting community was *Pelagibacter*, which accounted for 10% of assignable reads at 0 h. The vast majority of *Pelagibacter*–like sequences shared highest similarity to the *Pelagibacter ubique* HTCC7211 genome, a strain cultivated from the oligotrophic Sargasso Sea (Stingl et al., 2007). Metagenomic samples taken from 36 h indicated small increases in the relative abundance of a variety of heterotrophic groups in both HMWDOM and ProDOM relative to the control (Figure 2B). These groups were the OM60 gammaproteobacteria, Alteromonadales, Rhodobacterales, SAR116 and Flavobacteriales. DNA sequences from the SAR11 group increased in the ProDOM treatment by nearly 50% over the control, suggesting a preference for this DOM source.

Prochlorococcus and *Pelagibacter* appeared to be the most transcriptionally active taxa in our experiment, as indicated by the proportion of assignable reads belonging to these two groups in the 0h cDNA library (Figure 2A). cDNA libraries from subsequent time points indicated subtle changes in taxonomic activity over time in DOM enriched microcosms relative to the control. While these temporal sequence data

198 indicated only minor changes in taxonomic profiles in response to DOM perturbations
199 on this short timescale, changes in gene expression patterns within the ambient
200 microbial community at Station ALOHA were more pronounced. Figure 2C shows the
201 taxonomic association of differentially expressed NCBI-nr genes that were significantly
202 enriched (posterior probability of ≥ 0.9) in cDNA samples from the treatments relative
203 to the control at each time point, where significantly underrepresented genes were
204 excluded. From a taxonomic perspective, both treatments exhibited a similar temporal
205 trend in differential gene expression. Across the first three time points the majority of
206 differentially expressed transcripts were associated with *Prochlorococcus*. *Pelagibacter*
207 demonstrated rapid responses in both treatments, with more consistent activity
208 captured in the HMWDOM treatment, where there was an increase in differentially
209 expressed transcripts at 27 h. The later time points indicated increasing transcript
210 abundances from different heterotrophic taxa, particularly *Alteromonadales* and the
211 OM60 clade, and these signals were typically observed earlier in ProDOM relative to
212 HMWDOM. These taxonomic trends in differential gene expression mirrored the
213 microbial community growth and abundance patterns (Figure 1B-G), where
214 *Prochlorococcus*-like cells represented the majority of growth at earlier time points, but
215 not later. Combined with high β-glucosidase activity at 36 h (Figure 1H and 1I), these
216 independent methods of analysis support the hypothesis that a microbial succession in
217 growth and activity occurred in our treatments in response to DOM perturbations.
218 Abundant, oligotrophic taxa (*Prochlorococcus* and *Pelagibacter*) were observed to
219 rapidly respond to changes in the ambient DOM pool. In contrast, the opportunistic

heterotrophic taxa (OM60, Alteromonadales, etc.) appeared to gradually increase in abundance, and their transcriptional responses became more apparent in the latter stages of the incubation.

Taxon-specific responses to DOM perturbations inferred from genome-centric transcriptomic analyses

To gain additional insight into microbial community dynamics and the DOM substrate utilization patterns driving the microbial successions previously described, we performed differential gene expression analyses on changes in relative transcript abundance within specific taxonomic bins. We focused on those taxa with the greatest percentages of differentially expressed genes (relative to the control; Figure 2C), which were *Prochlorococcus*, *Pelagibacter*, and gammaproteobacteria from the OM60 clade.

Prochlorococcus

DOM enrichments induced specific, rapid changes in *Prochlorococcus* gene expression in biosynthetic pathways as supported by the significant differential expression (DE) of KEGG orthologs (KOs) that were enriched in treatments (Figure 3A). Both DOM additions appeared to trigger a burst in protein biosynthesis in *Prochlorococcus* as the vast majority of DE KOs in the pathways Ribosome and Translation factors occurred at the 2 h time point in both treatments (dataset S2 and S3). *Prochlorococcus* also exhibited an immediate and sustained increase in the DE of KOs from pathways involved in genome replication and cell division (Figure 3A). The expression of KOs from lipid and starch biosynthesis pathways was also significantly

more abundant in DOM-enriched microcosms, suggesting increased levels of membrane biogenesis and carbon storage (Figure 3A). The greater number of DE KO's for protein, cell division and lipid biosynthesis pathways in ProDOM, combined with their higher percent increase relative to the HMWDOM treatment indicates that the magnitude of response by *Prochlorococcus* at the level of gene expression was more pronounced for ProDOM (Figure 3A). These observations support the hypothesis (also supported by the flow cytometry data) that ProDOM contained a greater amount of labile DOM, despite the higher quantity of carbon supplied in the HMWDOM treatment (Figure 1A).

The *Prochlorococcus* population in the control microcosm appeared to dedicate a greater fraction of its transcriptome to nitrogen acquisition and assimilation relative to the treatments. KOs involved in nitrogen metabolism and transport pathways were significantly under-represented in treatment samples (Figure 3A), including but not limited to the ammonium assimilation protein glutamine synthetase, and both the permease and substrate binding subunits of the Urea ABC transporter. Additionally, transcripts encoding an ammonium transporter ortholog unassigned in KEGG, represented the only *Prochlorococcus* ortholog that was significantly underrepresented in both treatments at every time point (see Cluster 287, Datasets S2 and S3). These nitrogen acquisiton genes are highly expressed by *Prochlorococcus* as a nitrogen scavenging response to nitrogen stress in culture (Tolonen et al., 2006) and their underrepresentation in treatments could indicate that both DOM treatments provided a labile source of DON.

To obtain a better understanding of the DOM utilization patterns that contributed to the physiological responses observed in *Prochlorococcus*, the DE of orthologs belonging to auxiliary KEGG pathways (as opposed to core pathways involved in central metabolic processes) was examined in greater detail. The number of DE *Prochlorococcus* orthologs binned into these two pathway categories (auxiliary vs. core) is presented in table 2 and details regarding KEGG pathway assignments as core or auxiliary are presented in Supplementary Files 1 and 2. At 2 h, *Prochlorococcus* transcripts mapping to the KO D-amino acid oxidase exhibited an ~8-fold increase in both treatments relative to the control (Tables S1 and S2). This KO catalyzes the breakdown of D-amino acids into their corresponding oxo-acids and ammonium and its increased activity suggests a source of proteinaceous material common to both treatments, perhaps in the form of peptidoglycan. Breakdown of D-amino acids should directly correspond to an increase in glutamine and glutamate via GS-GOGAT ammonium assimilation (Muro-Pastor et al., 2005). An increase in cellular concentrations of glutamate is supported by the DE of a number of KOs involved in the biosynthesis of aspartate, proline and arginine - amino acids that use glutamate as a metabolic precursor (Tables S1 and S2). The enrichment of various DE orthologs encoding peptidases and proteases was also observed in treatment transcriptomes, suggesting *Prochlorococcus* was capable of the uptake and degradation of oligopeptides present in the DOM additions. Transcripts for five different *Prochlorococcus* proteases were exclusively enriched in the ProDOM treatment, and four of them were enriched at 2 h, indicating a rapid response to an influx of protein. These observations indicate that

286 the *Prochlorococcus*-derived DOM fraction we employed was richer in labile protein
287 material than HMWDOM derived from surface seawater, despite the large discrepancy
288 in organic carbon quantity (Figure 1A).

289 ***Pelagibacter***

290 Similar to *Prochlorococcus*, *Pelagibacter* also exhibited rapid changes in gene
291 expression in response to both HMWDOM and ProDOM enrichment. The majority of DE
292 KO's involved in protein biosynthesis pathways occurred at the 2 and 12 h time points in
293 both treatments (Figure3B, datasets S4 and S5). The *Pelagibacter* population also
294 demonstrated transcriptional growth signals in response to DOM perturbation (Figure
295 3B) with DE KOs falling into the categories of DNA replication proteins and Chromosome.

296 Also like *Prochlorococcus*, *Pelagibacter* cells responded to DOM addition by
297 decreasing the expression of orthologs involved in nitrogen acquisition. These include
298 DE KOs from the pathway Nitrogen metabolism (Figure3B, datasets S4 and S5), such as
299 the ammonium assimilation protein glutamine synthetase and two paralogs of the
300 glycine cleavage system T protein that could be involved in nitrogen acquisition via the
301 breakdown of methylated organic nitrogen substrates (Sun et al., 2011). Transporters
302 were significantly underrepresented in *Pelagibacter* in both DOM treatments (Figure
303 3B). The majority of these DE KOs and other DE transport orthologs unannotated in
304 KEGG were annotated in NCBI-nr as functioning in the uptake of organic or inorganic
305 nitrogen containing compounds (Tables S3-S6).

306 Similar to *Prochlorococcus,* the underrepresentation of *Pelagibacter* transcripts
307 related to nitrogen acquisition may also indicate that DOM additions provided a source
308 of organic nitrogen. To gain further insight into *Pelagibacter* DOM substrate utilization

we examined differentially expressed KOs belonging to auxiliary pathways outside of those core pathways involved in central metabolic processes (see Table 2 for ortholog counts and Supplementary file 2 for pathway designations). The gene encoding formate-tetrahydrofolate ligase (*fhs*) was significantly enriched in *Pelagibacter* transcripts from the HMWDOM treatment at the 27 h time point (Table S7) and was on average 62% higher than the control across all time points, suggesting an influx of C1 groups entering the tetrahydrofolate (THF) oxidation pathway. Whereas transporters were generally underrepresented in the treatments, a few transporters appeared to be stimulated by the DOM additions (Tables S5 and S6). In the HMWDOM treatment, we observed significant enrichment of transcripts for the gene encoding the PheC transporter (Table S5), which is linked to the sarcosine oxidase operon in multiple *Pelagibacter* genomes. The DE of *fhs* and *pheC* potentially link the uptake of methylated organic nitrogen compounds, like sarcosine, to C1 oxidation in *Pelagibacter,* providing a mechanism for nitrogen acquisition and the production of energy needed to fuel the growth signals observed in KEGG pathways (Figure 3B).

In the ProDOM treatment, two *Pelagibacter* orthologs involved in homocysteine biosynthesis were enriched at the 2 h time point (Table S8). These were homoserine O-acetyltransferase (*metX*) and O-acetylhomoserine (thiol)-lyase (*metY*). Homocysteine is required by the enzyme betaine-homocysteine methyltransferase (BHMT) for the first demethylation step in glycine betaine degradation (Barra et al., 2006). The gene encoding BHMT was not detected as differentially expressed over the entire course of the experiment (likely due to its low representation among SAR11 transcripts), however

its expression was 4-fold higher in ProDOM relative to the control at 2 h (posterior probability = 0.63). Transcripts for a gene annotated as γ-butryobetaine dioxygenase (*γ-bbh*) was enriched in ProDOM at 12 h and this protein catalyzes the first step in the degradation of γ-butryobetaine, a substance whose degradation results in the production of glycine betaine (Kleber, 1997). In the *Pelagibacter* HTCC7211 genome, homologs encoding subunits of a L-proline/glycine betaine ABC transporter are linked to the *γ-bbh* gene. Together these observations suggest that the ProDOM treatment provided a source of γ-butryobetaine- and glycine betaine-like substrates, thereby supplying *Pelagibacter* with a source of both nitrogen and energy.

OM60 Clade

Of the 3,666 OM60 clade ortholog clusters identified among the sequenced data (Dataset S1), 37 were detected as differentially expressed in cDNA samples from the HMWDOM treatment and 70 were detected from the ProDOM treatment. The vast majority of these DE orthologs occurred at the 27 and 36 h time points, and those enriched in treatments included orthologs from KEGG pathways involved in protein, nucleotide and peptidoglycan biosynthesis (Tables S9 and S10). These later time points also coincided with the growth of non-*Prochlorococcus* cell types in treatments as determined by flow cytometry data and increasing activity of β-glucosidase (Figure 1).

Interestingly, differentially expressed orthologs indicate OM60 polysaccharide utilization in both DOM treatments. Transcripts for a predicted beta-glucoside-specific TonB-receptor (cluster 4450) was enriched in both treatments at 27 and 36 h (Tables S9

and S10). In the HTCC2148 genome, this TonB receptor homolog is located downstream of a glycosyl hydrolase gene, which was significantly enriched in OM60 transcripts in the HMWDOM treatments at 27 h. Further examination of this glycosyl hydrolase (GH) homolog from the HTCC2148 genome using the database for Carbohydrate-active enzyme ANnotation (http://csbl.bmb.uga.edu/dbCAN/), found the signature catalytic motif EXDXXE of the GH16 family (http://www.cazypedia.org/index.php/Glycoside_Hydrolase_Family_16, Michel et al., 2001), which is also present in the transcripts mapping to this region of the gene in both treatments. Enzymes of the GH16 family are known to cleave β-1,3 linked glucans and galactans (Baumann et al., 2007; Hehemann et al., 2010), which are often abundant in HMWDOM (Aluwihare et al., 1997). GH16 enzymes preferentially hydrolyze longer-chain substrates, which could have provided the shorter oligosaccharides that induced β-glucosidase enzyme activity in the treatments (Figure 1G and H).

In accordance with signals for polysaccharide utilization and uptake, OM60 transcripts from the ProDOM treatment (Table S10) showed enrichment in genes encoding glycolysis (enolase and pyruvate kinase at 27 h) and citric acid cycle enzymes (isocitrate dehydrogenase and succinyl-CoA synthetase at 36 h). That similar signals were not observed in HMWDOM (Table S9) may indicate a slower response time in this treatment compared to ProDOM. This hypothesis is supported by the higher proportion of OM60 transcripts relative to the entire community in ProDOM cDNA samples at 27 and 36 h (Figure 2A) and the greater number of DE orthologs in this treatment. These observations once again suggest that the ProDOM amendment contained a higher

375 concentration of more labile substrates, which may have accelerated the rate at which
376 the heterotrophic population was able to respond.
377
378 **Discussion**
379 We investigated the response of an oligotrophic microbial community to two
380 organic carbon sources using controlled microcosm experiments in the North Pacific
381 Subtropical Gyre. Both treatments induced similar patterns in cell growth, taxonomic
382 response and exoenzyme activity despite differences in the quantity and quality of the
383 carbon added. These observations suggest that ProDOM contained a greater proportion
384 of labile carbon relative to HMWDOM, which represented a standing stock of semi-labile
385 and refractory organic carbon subjected to persistent heterotrophic activity. This
386 hypothesis is supported by transcriptional signals that indicate a stronger response to
387 ProDOM by *Prochlorococcus* and the OM60 clade.
388 Relative to the control, the *Prochlorococcus* transcriptional responses from
389 treatment microcosms indicated that DOM enrichments provided DON substrates in the
390 form of proteinaceous material, which appeared linked to an increase in gene
391 expression in biosynthetic pathways and a decrease in the expression of genes involved
392 in nitrogen acquisition. Studies have shown that *Prochlorococcus* utilizes various
393 nutrient acquisition strategies to circumvent nitrogen and phosphorus depletion
394 (Martiny et al., 2006; Martiny et al., 2009), and highlighted the ability of this
395 cyanobacterium to utilize organic nutrients for growth (Martínez et al., 2012; Gómez-
396 Pereira et al., 2013; del Carmen Muñoz-Marín et al., 2013). Some studies suggest that

the ecological success of *Prochlorococcus* in oligotrophic regions of the ocean is due in part to their high uptake rate of amino acids (Zubkov et al., 2004; Mary et al., 2008), which can account for 33% of the total bacterioplankton turnover of these compounds in oligotrophic parts of the Arabian Sea (Zubkov et al., 2003). These authors note that the classical distinction between auto- and hetero-trophic organisms in the marine environment is blurred in oligotrophic waters where photosynthetic cyanobacteria often demonstrate mixotrophic tendencies by utilizing organic nutrients.

Similar to the *Prochlorococcus* population, *Pelagibacter* transcriptional responses in the treatments also indicated the utilization of DON substrates. *Pelagibacter* transcriptional signals for the utilization of methylated organic nitrogen compounds in the treatments appeared linked to the enrichment of transcripts from genes involved in biosynthetic processes and the underrepresentation of genes involved in nitrogen acquisition. *Pelagibacter* is capable of the uptake and degradation of a wide variety of one-carbon compounds including methyl functional groups from methylated compounds, which provide a source of energy via the C1 tetrahydrofolate (THF) oxidation pathway (Sun et al., 2011). Our results suggested that in addition to an energy source, *Pelagibacter* could utilize methylated organic nitrogen compounds from the ambient DOM pool to acquire nitrogen. A metaproteomic study conducted in the euphotic zone of the seasonally phosphorus-limited Sargasso Sea found that the periplasmic substrate-binding protein for phosphonate acquisition was among the most frequently detected *Pelagibacter* proteins (Sowell et al., 2009), indicating that these organisms rely on the ambient DOM pool for survival under nutrient poor conditions.

OM60 clade transcripts in the treatment microcosms were significantly enriched relative to the control at later time points, and involved genes in polysaccharide degradation and various biosynthetic processes. Whereas abundant taxa like *Prochlorococcus* and *Pelagibacter* demonstrated rapid responses to DOM enrichment, the OM60 population represented a low abundance group that responded at later time points. Many studies show that opportunistic, low abundance taxa bloom under increasing concentrations of organic nutrients (Cottrell and Kirchman, 2000; Eilers et al., 2000; McCarren et al., 2010; Romera-Castillo et al., 2011; Tada et al., 2011; Nelson and Carlson, 2012). These opportunistic taxa exhibit a "feast or famine" lifestyle (Nissen, 1987; Flärdh et al., 1992; Srinivasan and Kjelleberg, 1998), and are often referred to as copiotrophs (Lauro et al., 2009; Yooseph et al., 2010). We suggest that oligotrophic conditions at Station ALOHA were likely responsible for the low abundance and activity of copiotrophs like members of the OM60 clade and that exposure to elevated concentrations of organic nutrients allowed this population to gradually increase in numbers such that their transcriptional responses became more apparent in the latter stages of the incubation.

McCarren *et al*. (2010) conducted a similar HMWDOM microcosm experiment within the mixed layer of the North Pacific Subtropical Gyre, however results from that study showed rapid and strong responses in copiotrophic taxa, particularly among organisms of the Alteromonadales. Differences in response dynamics between that study and the one presented here are likely the result of multiple variables. The McCarren *et al*. treatment had a DOC concentration that was 300% greater than

441 ambient conditions, more than double the amount of HMWDOM used here, and the
442 percent abundance of cDNA reads from Alteromonadales was 300% greater in the
443 starting community of that experiment relative to that observed in our experiments.
444 These two variables implicate a potential founder effect for an organism known to have
445 rapid growth kinetics under increasing substrate concentrations (Eilers et al., 2000).

446 A major challenge in microbial oceanography is to understand the mechanisms
447 driving changes in community composition and activity across temporal and seasonal
448 time scales (Fuhrman et al., 2006; Giovannoni and Vergin, 2012; Ottesen et al., 2013). In
449 areas where seasonal stratification of the water column regularly occurs (Karl et al.,
450 2012), an extremely oligotrophic microbial assemblage can result due to inorganic
451 nutrient depletion. Amendment of such an assemblage with two distinct DOM sources
452 indicated that numerically dominant oligotrophic microbes have the ability to rapidly
453 acquire nitrogen from organic sources and implicates the importance of carbohydrates
454 within the DOM pool for sustaining less abundant copiotrophic microorganisms in these
455 systems.

456 **Experimental procedures**

457 ***Experimental setup and sample collection***

458 Seawater for microcosm incubation experiments was collected at 22° 45'N, 158°
459 00'W from the bottom of the mixed layer (35 m) at dawn, on May 27, 2010. Hydrocasts
460 for sampling were conducted using a conductivity-temperature-depth (CTD) rosette
461 sampler aboard the R/V *Ka`imikai-o-Kanaloa*. Water was transferred to pre-acid-washed,
462 sample-water rinsed 20 L polycarbonate bottles. The deck-board incubator was a blue

light type, which simulated light levels at ca. 10m (roughly 35% surface irradiance). Twenty-liter carboys were wrapped in a single layer of black fiberglass screen, to further decrease the light level inside the carboys to 14% surface irradiance, the *in situ* light intensity at 25-45m. Carboys were incubated in deck-board incubators supplied with flow-through surface seawater to maintain near *in situ* temperatures. The control microcosm consisted of 20 L of 35 m water and for the treatments 2 L of DOM concentrate (HMWDOM or ProDOM) was added to 18L of water obtained from 35 m depth for a total volume of 20 L.

RNA and DNA sampling

At selected time points, bacterioplankton biomass from ~2 L of sample water was rapidly collected for RNA extraction by first pre-filtering through a 1.6 µm glass fiber filter and then harvesting cells onto 0.2 µm Sterivex (Millipore) filters. Filtration was limited to 10 minutes or less. 1.8 ml of RNAlater® (Applied Biosystems) was added to the filter, which was subsequently capped and flash frozen at -80 °C. Samples were transported frozen in a dry shipper and stored at -80 °C until RNA extraction procedures. At both the beginning and end of the experiment, biomass was similarly collected for DNA samples. 18 L of seawater for T0 DNA sample collection were directly taken from the CTD bottle (not from the microcosms) and 5-6 L of water were filtered from the end of the experiment for DNA extractions. Filter units for DNA extraction were filled with lysis buffer (50 mM Tris-HCl, 40 mM EDTA, and 0.75 M sucrose), capped and frozen at -20 °C until extraction.

RNA extraction

Total RNA was extracted using the *mir*Vana™ miRNA Isolation kit (Ambion) with modification to account for the recovery of RNA from Sterivex filters. Filters were thawed on ice, and at which point RNAlater® was expelled via syringe and discarded. 1.5 ml of Lysis/Binding Buffer was added to the filter, which was resealed and vigorously vortexed for 1 minute. 150 µl of miRNA Homogenate Additive was added, and after vortexing, the filter was incubated on ice for 10 minutes. The resulting lysate was removed with a syringe and divided into two 2ml tubes, which were processed separately through the remainder of the standard *mir*Vana™ miRNA Isolation kit protocol. Following purification of the total RNA from the *mir*Vana™ columns, samples resulting from a single filter were combined back together for genomic DNA removal with TURBO DNA-free™, then purified and concentrated using the RNeasy MinElute Cleanup kit (Qiagen).

DNA Isolation

Total DNA was extracted and purified using the Quick-Gene 610 l system (Fujifilm, Tokyo, Japan) and DNA Tissue Kit L with a modified lysis protocol. 50 mg of lysozyme was added to 1 ml of lysis buffer (described above), mixed by vortexing before 40 µl was added to thawed Sterivex filters. Filters were set in a rotating incubator at 37 °C for 45 min. Following this, 100 µl each of the kit buffers EDT and MDT were added to the filter, which was incubated at 55 °C for 2 h with rotation. The lysate was decanted from the filter using a syringe, 2 ml LDT solution was added to the lysate, mixed by inversion, and incubated at 55 °C for a further 15 min without rotation. 2.7 ml EtOH was added and vigorously mixed by vortexing, at which point the sample was immediatedly loaded onto

507 the QuickGene column and placed in the Quick-Gene 610 l instrument for purification
508 according to the manufacturer's DNA Tissue protocol, with an elution volume of 400 µl.

509 ***rRNA subtraction, RNA amplification, cDNA synthesis***

510 Ribosomal RNA transcripts were removed from total RNA extracts using a
511 subtractive hybridization protocol published in Stewart et al. (2010) with slight
512 modifications. Bacterial and archaeal 16S and 23S rRNA probes were separately
513 amplified from DNA sampled from 0h and 36h microcosm communities using 50 µl
514 Herculase II Fusion DNA Polymerase reactions and 30 ng of template DNA. PCR products
515 from these individual reactions for each subunit were pooled together for PCR
516 purification via the QIAquick PCR purification kit (Qiagen), eluted with 30 µl and DNA
517 was quantified using a ND-1000 spectrophotometer (Nandrop technologies). Each
518 elution was dried by speed vac (Savant) and concentrated to obtain the 250-500 ng
519 required for the *in vitro* transcription to generate biotin labeled anti-sense rRNA probes.
520 Hybridization reactions containing 150 ng of total community RNA was hybridized with
521 1200 ng of rRNA probe master mix, which was comprised of 450 ng each bacterial and
522 150 ng each archaeal small- and large-subunit rRNA probes. Probe removal was
523 performed as indicated in Stewart *et al.* (2010).

524 Purified and concentrated rRNA subtracted RNA was linearly amplified and
525 converted to cDNA using the MessageAmp™ II-Bacteria kit (Ambion) following the
526 manufacturer's instructions and as originally described in Frias-Lopez et al. (2008).
527 Samples containing 9 to 25 ng of RNA were polyadenylated using *Escherichia coli* poly(A)
528 polymerase I. Poly(A)-tailed RNA was reverse transcribed using the oligo(dT) primer T7-

BpmI-d$(T)_{16}$VN (5'-GCCAGTGAATTGTAATACGACTCACTATAGGGGCGACTGGAGTTTTTTTTT TTTTTTTVN-3'), which contains a promoter sequence for T7 RNA polymerase and a recognition site for the restriction enzyme *Bpm*I. cDNA templates were transcribed *in vitro* (37°C for 6h) resulting in µg quantities of antisense RNA (aRNA). The aRNA was the converted to double-stranded cDNA. First strand synthesis was performed using the SuperScript III First-Strand Synthesis System (Invitrogen) using random hexamer priming and second strand synthesis was accomplished using the SuperScript Double-Stranded cDNA synthesis kit (Invitrogen). cDNA was purified with the QIAquick PCR purification kit (Qiagen) before digestion with *Bpm*I for 3 hours at 37°C to remove poly(A)-tails, after which *Bpm*I was heat inactivated at 70°C for 20 minutes.

Pyrosequencing

Pyrosequencing was performed using Titanium series chemistry on a Roche Genome Sequencer FLX instrument. Library construction followed the Titanium Rapid Library Preparation protocol. To obtain a size distribution of cDNA molecules that also contained smaller fragments, adaptor-ligated libraries were not diluted before size selection with AMPure XP beads. Library concentrations were determined using the Titanium slingshot kit (Fluidigm) and added to emulsion PCR reactions at 0.1 molecules per bead. 454 Life Sciences (Roche) standard protocols were used for sequencing and quality controls. The sequences reported in this paper have been deposited in the NCBI sequence read archive under study SRP021115.

Flow Cytometry

At each time point, 5 µl of 25% grade 1 glutaraldehyde (Sigma) was added to 1 ml of seawater, mixed by inversion, incubated at room temperature for 10 minutes, then flash frozen in liquid N_2 and stored at -80 °C. Samples were thawed in the dark and cell counts were performed using an Influx cytometry platform (Becton Dickinson). *Prochlorococcus*-like cells were identified based on their unique red autofluorescence and scatter signals, using a 692 nm laser and vertical forward scatter. Prior to total cell counts, samples were stained with SYBR Green (Invitrogen, Carslbad CA) for 10 min, and DNA-containing cells were identified based on SYBR fluorescence using a 530 nm laser and scatter signals (Marie et al., 1997). A minimum of 20,000 *Prochlorococcus*-like cells and 35,000 SYBR stained cells were counted per sample, where the count error based on a Poisson distribution is less than 1% of counts. Flow cytometry count data was analyzed using FlowJo software (Tree Star).

Exoenzyme assay

β-glucosidase activity was measured as an increase in fluorescence of the product 4-Methylumbelliferone (MUF) released after enzymatic hydrolysis of the non-fluorescent 4-Methylumbelliferyl-β-D-glucopyranoside (MUF-Glc; Sigma-Aldrich) substrate. The kinetic parameters of β-glucosidase activity for each time point were measured in a series of eight different MUF-Glc concentrations, ranging from 0.05 to 100 µM (final concentration). The highest concentration (in this case, 100 µM) was saturating and was performed in triplicate for each sample individually. Summarized across all triplicate samples, the mean of the standard error was 1.4% and the standard

deviation of all the standard errors obtained was +/- 1.4% indicating low levels of variability.

The kinetic parameters were determined using the Hanes–Woolf plot graphical representation of the rearrangement of the Michaelis–Menten equation as follows: $S:V = K_m :V_m + S:V_m$, with the MUF-Glc concentration (S), the hydrolysis rate (V), the maximum hydrolysis rate (V_m), and the half-saturation constant (K_m). All samples were incubated in the dark at *in-situ* temperature in an incubator. Hydrolysis of MUF-Glc to MUF (excitation and emission: 359 and 449 nm, respectively) was measured on a Kontron SFM25 spectrofluorometer. At least four measurements were obtained within 18 h to verify the linearity of the assay. A standard curve using MUF (Sigma-Aldrich) from 0 to 500 nM in 0.2 µm-filtered and boiled seawater was used to calculate hydrolysis rates. Blanks (i.e., ultrapure water) and killed controls (i.e., sample fixed with 0.2% paraformaldehyde, final concentration) were run periodically at saturating concentration and indicated no significant autohydrolysis of the substrate.

Preparation of DOM amendments

High-molecular weight DOM was isolated and concentrated from surface seawater as described in McCarren *et al.* (2010) with the following modifications. 434 L of surface seawater was obtained using acid-cleaned Teflon tubing connected to a compressed air-driven diaphragm pump (Wilden) and concentrated 100-fold over a period of 36 h using a single thin-film ultrafiltration membrane element (Spearation Engineering) in a custom-built polycarbonate membrane housing. Samples were taken for TOC quantification, cell counts, and viral particle counts from the raw seawater, 0.2

593 µm filtrate, and permeate water periodically during ultrafiltration and from the
594 concentrate upon completion. This sample suite was also taken after serial filtration of
595 the concentrate through a 0.1 µm Polycap TC prefilter (Whatman) followed by a 30-kDa
596 polyethersulfone membrane (Millipore) to remove viral particles as described in
597 McCarren *et al.* (2010). Cell and viral counts determined pre- and post-30kDa filtration
598 using flow cytometry and fluorescence microscopy indicated the removal of cells, cell
599 debris, and the reduction of virus particles below ambient concentrations of seawater
600 from the mixed-layer at Station ALOHA (data not shown).

601 *Prochlorococcus*-derived DOM was isolated from an axenic culture of
602 *Prochlorococcus* strain MIT9313 grown in 20 L of Pro99 medium prepared according to
603 existing protocols (Moore et al., 2007) in sterile Sargasso seawater. The culture was
604 maintained at 22 ^{o}C and ca. 20 µmol photons/m^2/s and monitored for growth using bulk
605 fluorescence. Upon reaching stationary phase, cell biomass was removed by
606 centrifugation and 0.1 µm filtration (Whatman Polycap 36 TC capsule filter). Filtrate was
607 acidified to pH 2-3 by adding trace metal grade hydrochloric acid before loading onto a
608 custom packed column containing soxhlet purified octadecyl (C_{18}) functionalized silica
609 gel (Sigma-Aldrich) at a rate of 2 ml/min. The column was then washed with ultrapure
610 water (pH 2-3) at a flow rate of 1 ml/min to remove salts before eluting with 10 column
611 volumes of acidified HPLC-grade methanol (pH 2-3) at a rate of 1 ml/min. Salt removal
612 was confirmed using a silver nitrate solution and the methanol elution was concentrated
613 using a rotary evaporator. A subsample was taken for HPLC/MS analysis and the
614 remaining sample was dried using filtered high purity nitrogen gas, rinsed with ultrapure

615 water to remove residual methanol, and then dried again. Dried ProDOM material was
616 stored in a combusted amber vial in the dark prior to resuspension at sea in filtered (0.1
617 µm Polycap TC; Whatman) seawater collected from 35 m at Station ALOHA.

618 ***Quantification of organic carbon and dissolved nitrogen***

619 Total organic carbon (TOC) and total dissolved nitrogen (TDN) were measured
620 using the high temperature combustion method on a Shimadzu TOC-V_{CSH} with platinized
621 aluminum catalyst coupled to a TNM-1 total nitrogen detector, while particulate organic
622 carbon (POC) was measured at the University of California Davis Stable Isotope Facility.
623 Details regarding sample handling and processing are provided in Supplementary File 1.

624 ***Chromatographic separation and detection of MIT9313 metabolites***

625 Chromatographic separation and detection of metabolites derived from
626 *Prochlorococcus* strain MIT9313 was achieved using an Agilent 1200 series liquid
627 chromatograph coupled to an Agilent 6130 mass spectrometer with an atmospheric
628 electrospray ionization source. Mass spectral data was acquired from 100-2000 Da in
629 the positive mode and ions with minimum signal intensity 5-fold greater than the
630 maximum noise level were included in analysis. Details regarding run conditions and
631 feature detection are provided in Supplementary File 1.

632 ***Bioinformatics***

633 Metagenomic and metatranscriptomic sequences derived from rRNA were
634 identified using BLASTN with a bit score cutoff of 50 against a database composed of 5S,
635 16S, 18S, 23S and 28S rRNA sequences from microbial genomes and the SILVA LSU and
636 SSU databases (http://www.arb-silva.de). Reads with best BLASTN hits to rRNA averaged

637 0.5% and 31% in DNA and cDNA libraries respectively, and these sequences were
638 excluded from further analyses. Non-rRNA sequences with identical start sites (first 3
639 bp), 99% identity and ≤1-bp length difference were identified as probable artificially
640 duplicated sequences (Stewart et al., 2010) and removed using the cd-hit program (Li
641 and Godzik, 2006) and scripts developed in (Gomez-Alvarez et al., 2009). Non-rRNA
642 sequences were compared with the 31 May 2010 version of NCBI's non-redundant (nr)
643 protein reference database using BLASTX, and a bit score cutoff of 50 was used to
644 identify significant matches. The MEGAN program (Huson et al., 2007) was used to
645 assign sequences to a higher-order taxonomy where sequences were assigned to the
646 lowest common ancestor of a set of taxa if the bit scores of any database matches were
647 within 3% of the top-scoring hit. The number of reads with significant matches to
648 different taxonomic orders was normalized according to the total number of all
649 significant hits to the NCBI nr database for an individual sample.

650 To identify NCBI-nr reference genes with statistically significant read counts we
651 used baySeq, a Bayesian method for identifying differential gene expression between
652 samples (Hardcastle and Kelly, 2010). The differential expression of reference genes
653 (posterior probability of $\geq$ 0.9) at the both the whole community and taxon-specific
654 levels were determined between treatment and control metatranscriptomes for each
655 time point individually (see Supplementary File 1 for further details).

656 Using the method published in Ottesen et al. (2013), taxon-specific ortholog
657 sequence clusters were generated separately for *Prochlorococcus*, *Pelagibacter*, and the
658 OM60 clade using sequenced genome representatives from NCBI. Within each taxon bin,

659 transcript counts for genes shared between multiple reference genomes of the same
660 taxa were combined into ortholog counts annotated with KEGG pathway information
661 (see Supplementary File 1 for further details). This approach was implemented to avoid
662 artificial division of transcript pools from environmental organisms among multiple,
663 imperfectly matched reference sequences (Ottesen et al., 2013). Analyses of
664 transcriptional dynamics focused on changes in relative transcript abundance within
665 each specific taxonomic bin. Significant DE of KEGG annotated orthologs (Datasets S2-
666 S5) was used to direct and support comparisons of taxon-specific pathway abundances
667 through time. In some cases, non-significant orthologs are discussed in taxon specific
668 analyses as supporting information. Differentially expressed orthologs were further
669 binned into central or auxiliary pathways (for specific details see Supplementary File 1).
670 Heatmaps (Figure 3) were generated in R using the heatmap.2 function in gplots
671 (Warnes et al., 2009).
672
673 **Acknowledgements**
674 The authors would like to thank the cruise chief scientist S. Wilson and the captain and
675 crew of the R/V *Ka`imikai-o-Kanaloa* for their help in collecting samples for this study.
676 Our gratitude goes to R. Barry and T. Palden for all their hard work in preparing libraries
677 for pyrosequencing and to J. Eppley for his great work on the DeLong lab sequencing
678 pipeline. Many thanks to the Chisholm lab: P. Berube for providing spent
679 *Prochlorococcus* medium for ProDOM extraction and A. Coe, J. Thompson and S.
680 Roggensack for flow cytometry training. We thank C. Johnson for assistance with
681 chromatographic and spectrometric data acquisition, M. Nieto-Cid for help with

TOC/TDN analysis, and J-H. Hehemann for annotation of the OM60 glycosyl hydrolase and informative discussion. Thanks to L.A. Ventouras, C. Young, A. Martinez, F. Stewart and Y. Shi for valuable scientific discussions. This work is a contribution from the Center for Microbial Oceanography: Research and Education (C-MORE). This work was supported by a National Science Foundation Science and Technology Center Award EF0424599 (E.F.D. and D.M.K.), grants to D.M.K., D.J.R and E.F.D from the Gordon and Betty Moore Foundation, a gift from the Agouron Institute (to E.F.D.), and a fellowship (202180) to AKS from the Canadian Institutes of Health Research (CIHR).

References

Aluwihare, L.I., Repeta, D.J., and Chen, R.F. (1997) A major biopolymeric component to dissolved organic carbon in surface sea water. *Nature* **387**: 166-169.

Aluwihare, L.I., Repeta, D.J., and Chen, R.F. (1999) A comparison of the chemical characteristics of oceanic DOM and extracellular DOM produced by marine algae. *Marine Ecology Progress Series* **186**: 105-117.

Aluwihare, L.I., Repeta, D.J., Pantoja, S., and Johnson, C.G. (2005) Two chemically distinct pools of organic nitrogen accumulate in the ocean. *Science* **308**: 1007-1010.

Azam, F. (1998) Microbial control of oceanic carbon flux: the plot thickens. *SCIENCE-NEW YORK THEN WASHINGTON-* : 694-695.

Barra, L., Fontenelle, C., Ermel, G., Trautwetter, A., Walker, G.C., and Blanco, C. (2006) Interrelations between glycine betaine catabolism and methionine biosynthesis in Sinorhizobium meliloti strain 102F34. *J Bacteriol* **188**: 7195-7204.

Baumann, M.J., Eklöf, J.M., Michel, G., Kallas, M., Teeri, T.T., Czjzek, M., and Brumer, H. (2007) Structural evidence for the evolution of xyloglucanase activity from xyloglucan endo-transglycosylases: biological implications for cell wall metabolism. *The Plant Cell Online* **19**: 1947-1963.

Bertlisson, S., Berglund, O., Pullin, M.J., and Chisholm, S.W. (2005) Release of dissolved organic matter by Prochlorococcus. *Vie et Milieu* **55**: 225-232.

709 Carlson, C.A. (2002) Production and removal processes, In *Biogeochemistry of*
710 *marine dissolved organic matter.* Hansell, D.A. (eds). Academic Press, pp. 91-152.
711 Cottrell, M.T., and Kirchman, D.L. (2000) Natural assemblages of marine
712 proteobacteria and members of the Cytophaga-Flavobacter cluster consuming low-
713 and high-molecular-weight dissolved organic matter. *Appl Environ Microbiol* **66**:
714 1692-1697.
715 del Carmen Muñoz-Marín, M., Luque, I., Zubkov, M.V., Hill, P.G., Diez, J., and García-
716 Fernández, J.M. (2013) Prochlorococcus can use the Pro1404 transporter to take up
717 glucose at nanomolar concentrations in the Atlantic Ocean. *Proceedings of the*
718 *National Academy of Sciences* **110**: 8597-8602.
719 del Giorgio, P.A., and Duarte, C.M. (2002) Respiration in the open ocean. *Nature* **420**:
720 379-384.
721 Eilers, H., Pernthaler, J., and Amann, R. (2000) Succession of pelagic marine bacteria
722 during enrichment: a close look at cultivation-induced shifts. *Applied and*
723 *environmental microbiology* **66**: 4634-4640.
724 Field, C.B., Behrenfeld, M.J., Randerson, J.T., and Falkowski, P. (1998) Primary
725 production of the biosphere: integrating terrestrial and oceanic components. *Science*
726 **281**: 237-240.
727 Flärdh, K., Cohen, P.S., and Kjelleberg, S. (1992) Ribosomes exist in large excess over
728 the apparent demand for protein synthesis during carbon starvation in marine
729 Vibrio sp. strain CCUG 15956. *J Bacteriol* **174**: 6780-6788.
730 Frias-Lopez, J., Shi, Y., Tyson, G.W., Coleman, M.L., Schuster, S.C., Chisholm, S.W., and
731 DeLong, E.F. (2008) Microbial community gene expression in ocean surface waters.
732 *Proceedings of the National Academy of Sciences* **105**: 3805-3810.
733 Fuhrman, J.A., Hewson, I., Schwalbach, M.S., Steele, J.A., Brown, M.V., and Naeem, S.
734 (2006) Annually reoccurring bacterial communities are predictable from ocean
735 conditions. *Proc Natl Acad Sci U S A* **103**: 13104-13109.
736 Giovannoni, S.J., and Vergin, K.L. (2012) Seasonality in ocean microbial communities.
737 *Science* **335**: 671-676.
738 Gomez-Alvarez, V., Teal, T.K., and Schmidt, T.M. (2009) Systematic artifacts in
739 metagenomes from complex microbial communities. *ISME J* **3**: 1314-1317.

740 Gómez-Pereira, P.R., Hartmann, M., Grob, C., Tarran, G.A., Martin, A.P., Fuchs, B.M., et
741 al. (2013) Comparable light stimulation of organic nutrient uptake by SAR11 and
742 Prochlorococcus in the North Atlantic subtropical gyre. *ISME J* **7**: 603-614.
743 Hansell, D.A., Carlson, C.A., Repeta, D.J., and Schlitzer, R. (2009) Dissolved organic
744 matter in the ocean: a controversy stimulates new insights. .
745 Hardcastle, T.J., and Kelly, K.A. (2010) baySeq: empirical Bayesian methods for
746 identifying differential expression in sequence count data. *BMC Bioinformatics* **11**:
747 422.
748 Hehemann, J.H., Correc, G., Barbeyron, T., Helbert, W., Czjzek, M., and Michel, G.
749 (2010) Transfer of carbohydrate-active enzymes from marine bacteria to Japanese
750 gut microbiota. *Nature* **464**: 908-912.
751 Huson, D.H., Auch, A.F., Qi, J., and Schuster, S.C. (2007) MEGAN analysis of
752 metagenomic data. *Genome research* **17**: 377-386.
753 Johnson, Z.I., Zinser, E.R., Coe, A., McNulty, N.P., Woodward, E.M., and Chisholm, S.W.
754 (2006) Niche partitioning among Prochlorococcus ecotypes along ocean-scale
755 environmental gradients. *Science* **311**: 1737-1740.
756 Karl, D.M., and Lukas, R. (1996) The Hawaii Ocean Time-series (HOT) program:
757 Background, rationale and field implementation. *Deep Sea Research Part II: Topical*
758 *Studies in Oceanography* **43**: 129-156.
759 Karl, D.M., Bidigare, R.R., Church, M.J., Dore, J.E., Letelier, R.M., Mahaffey, C., and Zehr,
760 J. (2008) The nitrogen cycle in the North Pacific Trades biome: an evolving paradigm.
761 *Nitrogen in the Marine Environment* : 705-769.
762 Karl, D.M., Church, M.J., Dore, J.E., Letelier, R.M., and Mahaffey, C. (2012) Predictable
763 and efficient carbon sequestration in the North Pacific Ocean supported by
764 symbiotic nitrogen fixation. *Proc Natl Acad Sci U S A* **109**: 1842-1849.
765 Kleber, H.P. (1997) Bacterial carnitine metabolism. *FEMS microbiology letters* **147**:
766 1-9.
767 Kujawinski, E.B., Longnecker, K., Blough, N.V., Vecchio, R.D., Finlay, L., Kitner, J.B.,
768 and Giovannoni, S.J. (2009) Identification of possible source markers in marine
769 dissolved organic matter using ultrahigh resolution mass spectrometry. *Geochimica*
770 *et Cosmochimica Acta* **73**: 4384-4399.

771 Landa, M., Cottrell, M.T., Kirchman, D.L., Blain, S., and Obernosterer, I. (2013)
772 Changes in bacterial diversity in response to dissolved organic matter supply in a
773 continuous culture experiment. *Aquatic Microbial Ecology* **69**: 157-168.
774 Lauro, F.M., McDougald, D., Thomas, T., Williams, T.J., Egan, S., Rice, S., et al. (2009)
775 The genomic basis of trophic strategy in marine bacteria. *Proc Natl Acad Sci U S A*
776 **106**: 15527-15533.
777 Li, W., and Godzik, A. (2006) Cd-hit: a fast program for clustering and comparing
778 large sets of protein or nucleotide sequences. *Bioinformatics* **22**: 1658-1659.
779 Marie, D., Partensky, F., Jacquet, S., and Vaulot, D. (1997) Enumeration and Cell Cycle
780 Analysis of Natural Populations of Marine Picoplankton by Flow Cytometry Using
781 the Nucleic Acid Stain SYBR Green I. *Appl Environ Microbiol* **63**: 186-193.
782 Martiny, A.C., Coleman, M.L., and Chisholm, S.W. (2006) Phosphate acquisition genes
783 in Prochlorococcus ecotypes: evidence for genome-wide adaptation. *Proc Natl Acad*
784 *Sci U S A* **103**: 12552-12557.
785 Martiny, A.C., Kathuria, S., and Berube, P.M. (2009) Widespread metabolic potential
786 for nitrite and nitrate assimilation among Prochlorococcus ecotypes. *Proc Natl Acad*
787 *Sci U S A* **106**: 10787-10792.
788 Martínez, A., Osburne, M.S., Sharma, A.K., DeLong, E.F., and Chisholm, S.W. (2012)
789 Phosphite utilization by the marine picocyanobacterium Prochlorococcus MIT9301.
790 *Environ Microbiol* **14**: 1363-1377.
791 Mary, I., Garczarek, L., Tarran, G.A., Kolowrat, C., Terry, M.J., Scanlan, D.J., et al.
792 (2008) Diel rhythmicity in amino acid uptake by Prochlorococcus. *Environ Microbiol*
793 **10**: 2124-2131.
794 McCarren, J., Becker, J.W., Repeta, D.J., Shi, Y., Young, C.R., Malmstrom, R.R., et al.
795 (2010) Microbial community transcriptomes reveal microbes and metabolic
796 pathways associated with dissolved organic matter turnover in the sea. *Proc Natl*
797 *Acad Sci U S A* **107**: 16420-16427.
798 McCarren, J., Becker, J.W., Repeta, D.J., Shi, Y., Young, C.R., Malmstrom, R.R., et al.
799 (2010) Microbial community transcriptomes reveal microbes and metabolic
800 pathways associated with dissolved organic matter turnover in the sea. *Proc Natl*
801 *Acad Sci U S A* **107**: 16420-16427.

802 Michel, G., Chantalat, L., Duee, E., Barbeyron, T., Henrissat, B., Kloareg, B., and
803 Dideberg, O. (2001) The kappa-carrageenase of P. carrageenovora features a tunnel-
804 shaped active site: a novel insight in the evolution of Clan-B glycoside hydrolases.
805 *Structure* **9**: 513-525.
806 Moore, L.R., Coe, A., Zinser, E.R., Saito, M.A., Sullivan, M.B., Lindell, D., et al. (2007)
807 Culturing the marine cyanobacterium Prochlorococcus. *Limnol. Oceanogr. Methods*
808 **5**: 353-362.
809 Mopper, K., Stubbins, A., Ritchie, J.D., Bialk, H.M., and Hatcher, P.G. (2007) Advanced
810 instrumental approaches for characterization of marine dissolved organic matter:
811 extraction techniques, mass spectrometry, and nuclear magnetic resonance
812 spectroscopy. *Chem Rev* **107**: 419-442.
813 Muro-Pastor, M.I., Reyes, J.C., and Florencio, F.J. (2005) Ammonium assimilation in
814 cyanobacteria. *Photosynthesis Research* **83**: 135-150.
815 Nelson, C.E., and Carlson, C.A. (2012) Tracking differential incorporation of
816 dissolved organic carbon types among diverse lineages of Sargasso Sea
817 bacterioplankton. *Environmental Microbiology* **14**: 1500-1516.
818 Nissen, H. (1987) Long term starvation of a marine bacterium,< i> Alteromonas
819 denitrificans, isolated from a Norwegian fjord. *FEMS Microbiology Letters* **45**: 173-
820 183.
821 Ottesen, E.A., Young, C.R., Eppley, J.M., Ryan, J.P., Chavez, F.P., Scholin, C.A., and
822 Delong, E.F. (2013) Pattern and synchrony of gene expression among sympatric
823 marine microbial populations. *Proc Natl Acad Sci U S A* **110**: E488-E497.
824 Partensky, F., Hess, W.R., and Vaulot, D. (1999) Prochlorococcus, a marine
825 photosynthetic prokaryote of global significance. *Microbiol Mol Biol Rev* **63**: 106-127.
826 Poretsky, R.S., Sun, S., Mou, X., and Moran, M.A. (2010) Transporter genes expressed
827 by coastal bacterioplankton in response to dissolved organic carbon. *Environ*
828 *Microbiol* **12**: 616-627.
829 Rinta-Kanto, J.M., Sun, S., Sharma, S., Kiene, R.P., and Moran, M.A. (2012) Bacterial
830 community transcription patterns during a marine phytoplankton bloom. *Environ*
831 *Microbiol* **14**: 228-239.

832 Romera-Castillo, C., Sarmento, H., Alvarez-Salgado, X.A., Gasol, J.M., and Marrasé, C.
833 (2011) Net production and consumption of fluorescent colored dissolved organic
834 matter by natural bacterial assemblages growing on marine phytoplankton exudates.
835 *Appl Environ Microbiol* **77**: 7490-7498.
836 Sarmento, H., and Gasol, J.M. (2012) Use of phytoplankton-derived dissolved organic
837 carbon by different types of bacterioplankton. *Environ Microbiol* **14**: 2348-2360.
838 Sowell, S.M., Wilhelm, L.J., Norbeck, A.D., Lipton, M.S., Nicora, C.D., Barofsky, D.F., et
839 al. (2009) Transport functions dominate the SAR11 metaproteome at low-nutrient
840 extremes in the Sargasso Sea. *ISME J* **3**: 93-105.
841 Srinivasan, S., and Kjelleberg, S. (1998) Cycles of famine and feast: the starvation
842 and outgrowth strategies of a marineVibrio. *Journal of biosciences* **23**: 501-511.
843 Stewart, F.J., Ottesen, E.A., and DeLong, E.F. (2010) Development and quantitative
844 analyses of a universal rRNA-subtraction protocol for microbial
845 metatranscriptomics. *ISME J* **4**: 896-907.
846 Stingl, U., Tripp, H.J., and Giovannoni, S.J. (2007) Improvements of high-throughput
847 culturing yielded novel SAR11 strains and other abundant marine bacteria from the
848 Oregon coast and the Bermuda Atlantic Time Series study site. *ISME J* **1**: 361-371.
849 Sun, J., Steindler, L., Thrash, J.C., Halsey, K.H., Smith, D.P., Carter, A.E., et al. (2011)
850 One carbon metabolism in SAR11 pelagic marine bacteria. *PLoS One* **6**: e23973.
851 Tada, Y., Taniguchi, A., Nagao, I., Miki, T., Uematsu, M., Tsuda, A., and Hamasaki, K.
852 (2011) Differing growth responses of major phylogenetic groups of marine bacteria
853 to natural phytoplankton blooms in the western North Pacific Ocean. *Applied and*
854 *environmental microbiology* **77**: 4055-4065.
855 Teeling, H., Fuchs, B.M., Becher, D., Klockow, C., Gardebrecht, A., Bennke, C.M., et al.
856 (2012) Substrate-controlled succession of marine bacterioplankton populations
857 induced by a phytoplankton bloom. *Science* **336**: 608-611.
858 Tolonen, A.C., Aach, J., Lindell, D., Johnson, Z.I., Rector, T., Steen, R., et al. (2006)
859 Global gene expression of Prochlorococcus ecotypes in response to changes in
860 nitrogen availability. *Molecular Systems Biology* **2**.
861 Warnes, G.R., Bolker, B., and Lumley, T. (2009) gplots: Various R programming tools
862 for plotting data. *R package version* **2**.

863 Yooseph, S., Nealson, K.H., Rusch, D.B., McCrow, J.P., Dupont, C.L., Kim, M., et al.
864 (2010) Genomic and functional adaptation in surface ocean planktonic prokaryotes.
865 *Nature* **468**: 60-66.
866 Zubkov, M.V., Fuchs, B.M., Tarran, G.A., Burkill, P.H., and Amann, R. (2003) High rate
867 of uptake of organic nitrogen compounds by Prochlorococcus cyanobacteria as a key
868 to their dominance in oligotrophic oceanic waters. *Appl Environ Microbiol* **69**: 1299-
869 1304.
870 Zubkov, M.V., Tarran, G.A., and Fuchs, B.M. (2004) Depth related amino acid uptake
871 by Prochlorococcus cyanobacteria in the Southern Atlantic tropical gyre. *FEMS*
872 *Microbiol Ecol* **50**: 153-161.
873

874 **Figure Legends**

875

876 **Figure 1.** Microbial community dynamics determined by flow cytometry and β-
877 glucosidase exoenzyme assays. A) Shows the percent increase over ambient seawater
878 concentration of DOC and DON in microcosm perturbation experiments. For absolute
879 concentrations and their standard deviations see main text. Panels B) HMWDOM and C)
880 ProDOM show total community cell counts, while panels D) HMWDOM and E) ProDOM
881 show *Prochlorococcus*-like cell counts. Panels F) HMWDOM and G) ProDOM show
882 *Prochlorococcus*-like cell growth as a percentage of total community growth that
883 occurred within each of these treatments between consecutive time points. Panels H)
884 and I) plot the cell specific β-glucosidase activity for control and treatment microcosm
885 communities through time.

886

887 **Figure 2.** NCBI order level taxonomy of DNA and cDNA reads through time. A)
888 Proportion of the total number of assignable reads represented by a taxonomic order in
889 DNA and cDNA libraries. Only those groups that represented >3% of assignable reads
890 are shown B) The same as in A but only for selected heterotrophic taxa C) The
891 taxonomic association of those NCBI-nr genes detected as enriched in cDNA from
892 treatments relative to controls at each time point show which taxa exhibited changes in
893 gene expression in response to DOM addition. The numbers in brackets along the x-axis
894 denote the total number of NCBI-nr genes detected as significantly enriched in the
895 treatment at each time point. All taxa shown in A) are present in C) with the exception
896 of Caudovirales. Taxonomic representation of reads at the order level was chosen to

visually reduce the number of taxa represented on the plots, while simultaneously represent genomes from key divisions.

Figure 3. Heatmaps depicting the relative abundance of metabolic pathways in the metatranscriptome of various taxonomic groups over time for both DOM treatments. Pathway abundances for cDNA reads from each sample were calculated as a fraction of sequences mapping to a pathway over the total number of cDNA hits for a particular taxon with a significant match in KEGG. Level 3 pathway abundance is calculated as the percent change in the treatment relative to the control (% treatment – % control / % control), such that a value of 1 in the heatmap represents a 100% increase in a pathway in the treatment relative to the control. The dendrogram clusters pathways by similar mean abundance values. Note that all time points occurred during daylight hours. A) *Prochlorococcus* transcriptome. Only those pathways that have significant differentially expressed KOs that were either enriched or underrepresented in both treatments relative to the control in at least 3 of the 4 time points are shown. B) *Pelagibacter* transcriptome. The criteria for choosing pathways to display for *Pelagibacter* was slightly different from *Prochlorococcus*, in that only one treatment had to have DE KOs at 3 of 4 time points, rather than both. This was due to the decreased sequencing depth in *Pelagibacter*. Conflicting pathways that contained differentially expressed KOs that were both enriched and underrepresented in treatments at 3 of 4 time points are excluded. The clusters indicated by the black dots represent pathways enriched in the treatment by these criteria, and the remainder are those that were underrepresented. The numbers in brackets next to the pathway names (x/y) indicate the total sum of KOs

920 detected as differentially expressed (x) over the total number of KOs detected in that
921 pathway (y) across all time points for HMWDOM (orange) and ProDOM (green). Note
922 that DE KOs are sometimes assigned to multiple pathways encoding similar metabolic
923 functions (e.g. DNA replication proteins and Chromosome). Therefore, combining the
924 number of DE KOs from two pathways does not always equal the sum of the numbers in
925 brackets.

926
927
928
929

Figure 1.

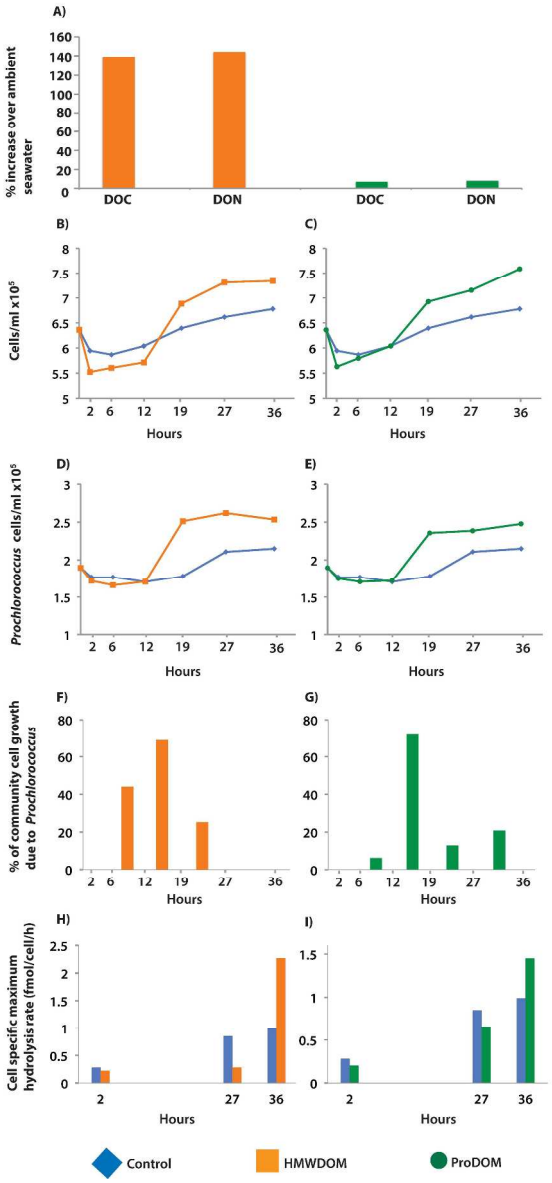

244x432mm (300 x 300 DPI)

Figure 2.

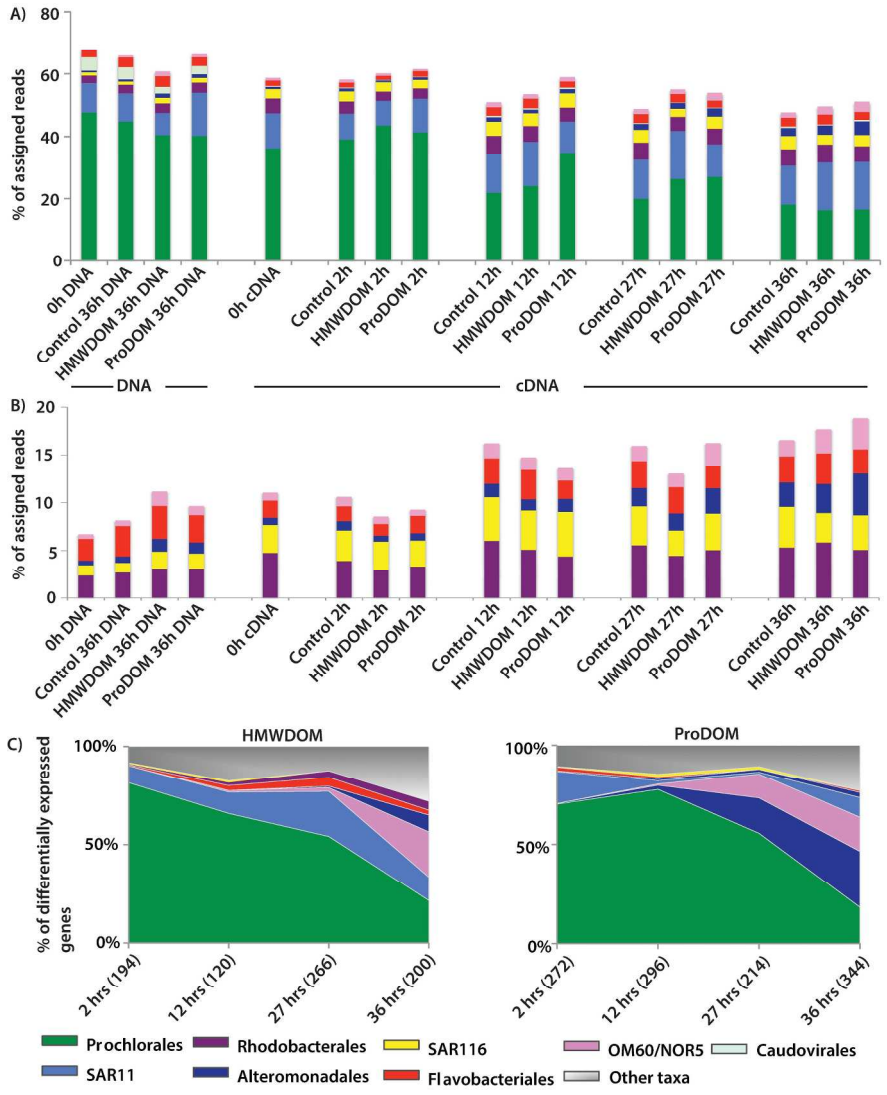

227x259mm (300 x 300 DPI)

Figure 3.

A) *Prochlorococcus*

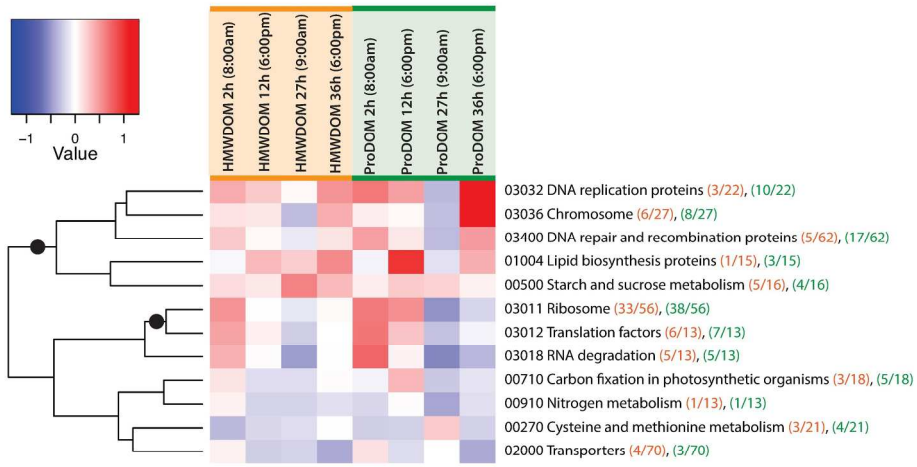

B) *Pelagibacter*

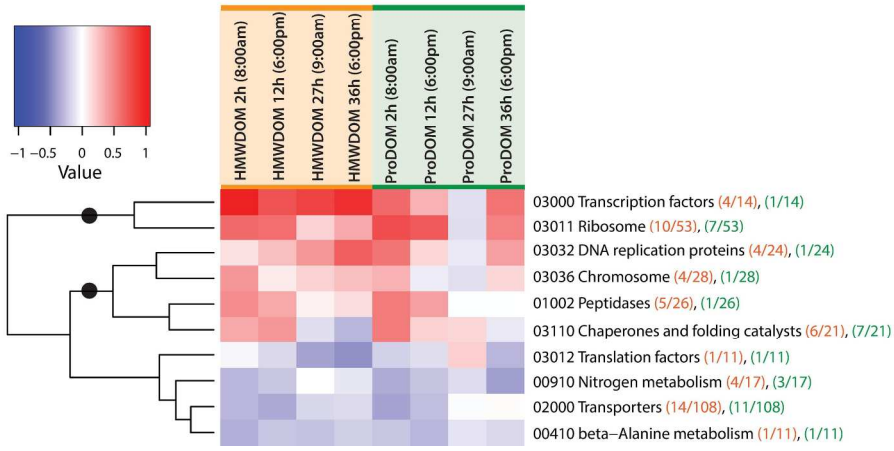

218x232mm (300 x 300 DPI)

Table 1. Read numbers and statistics

cDNA sample	Total reads[1]	Non-rRNA reads[2]	% rRNA[3]	NCBI hits[4]
0h	618918	369456	38.2	249185
Control 2h	711088	411428	38.6	298271
Control 12h	616224	431332	28.4	294160
Control 27h	593531	406165	30.2	261611
Control 36h	602581	417565	29.3	255126
HMWDOM 2h	556200	308146	42.4	194588
HMWDOM 12h	564333	401107	27.6	278836
HMWDOM 27h	534137	456035	14.0	314063
HMWDOM 36h	573227	462651	18.4	297466
ProDOM 2h	654338	472796	26.3	357097
ProDOM 12h	647187	255872	57.8	176581
ProDOM 27h	638776	432165	30.5	323866
ProDOM 36h	585229	439791	23.1	289130
DNA sample	Total reads	Non-rRNA reads	% rRNA	NCBI hits
0h	594218	591180	0.49	389357
Control 36	638559	635073	0.50	430104
HMWDOM 36	696659	692255	0.51	467678
ProDOM 36	618145	614493	0.52	452396

[1]Total number of sequence reads per run.
[2] Number of sequence reads after removal of rRNA sequences.
[3] The percentage of the total number of sequenced reads that had a best BLASTN hit to rRNA.
[4]Non-replicate, non-rRNA reads with a significant BLASTX hits to proteins in the NCBI non-redundant database.

Table 2. Number of *Prochlorococcus* and *Pelagibacter* ortholog clusters detected as differentially expressed (DE) in cDNA samples[1]

Organism and Treatment	Total DE + [2]	Core DE +[3]	Auxiliary DE +[4]	Unassigned DE +[5]	Total DE –	Core DE –	Auxiliary DE –	Unassigned DE –
Prochlorococcus HMWDOM	301/2743	114 (38%)	23 (8%)	164 (54%)	130/2743	72 (55%)	11 (9%)	47 (36%)
Prochlorococcus ProDOM	444 /2743	174 (39%)	35 (8%)	235 (53%)	211/2743	113 (54%)	22 (10%)	76 (36%)
Pelagibacter HMWDOM	100/1950	50 (50%)	17 (17%)	33 (33%)	46/1950	25 (55%)	2 (4%)	19 (41%)
Pelagibacter ProDOM	63/1950	32 (51%)	9 (14%)	22 (35%)	44/1950	23 (52%)	3 (7%)	18 (41%)

[1]The total number of ortholog clusters detected in all cDNA samples was 2734 for *Prochlorococcus* and 1950 for *Pelagibacter*. Those orthologs that were enriched in treatments relative to controls are indicated by + and those that were underrepresented as –. The number of ortholog clusters detected as DE in *Pelagibacter* is lower due to decreased sequencing depth compared to *Prochlorococcus*.

[2]Total DE refers to the total number of orthologs detected as DE as either enriched (+) in treatments relative to controls, or underrepresented (–)

[3]Core DE refers to the total number of orthologs detected as DE in a core pathway involved in central metabolic processes and the number in brackets represents their fraction of total DE orthologs

[4]Auxiliary DE refers to the total number of orthologs detected as DE in an auxiliary pathway and the number in brackets represents their fraction of total DE orthologs

[5]Unassigned DE refers to the total number of DE orthologs that were not assigned to KEGG level 3 pathways and the number in brackets represents their fraction of total DE orthologs

Supplementary file 1

Includes: Supplemental experimental procedures, Figure S1 and Tables S1-S12.

Experimental procedures

Quantification of organic carbon and dissolved nitrogen.

Combusted glassware (450 ^{o}C for 8 h) was used for all sampling. Sub-samples of 30 ml for total organic carbon (TOC) and total dissolved nitrogen (TDN) were transferred into glass vials and acidified with 150 µl of a 25% phosphoric acid solution before sealing with acid-washed Teflon lined septa and storage in the dark at 4 ^{o}C until processing. Sample concentrations were determined using the high temperature combustion method alongside potassium hydrogen phthalate and potassium nitrate standards and consensus reference materials provided by the DOC-CRM program (www.rsmas.miami.edu/groups/biogeochem/CRM.html). Particulate organic carbon (POC) analysis of solid-phase extracted *Prochlorococcus*-derived material was measured by placing 50 µl of sample onto a combusted 25 mm 0.7 µm glass fiber filter (Whatman GF/F) and allowing methanol to evaporate in a chemical hood. Filters were then placed inside a combusted glass petri dish, wrapped in foil, and immediately frozen. This process was repeated to obtain duplicate samples and blank filters with 50 µl of pure methanol added were also prepared. Filters were later thawed and put in a drying oven (60 ^{o}C) overnight to ensure they were thoroughly dried before encapsulation into 9x10 mm tin capsules and shipped to the University of California Davis Stable Isotope Facility for quantification.

Chromatographic separation and detection of MIT9313 metabolites.

Chromatographic separation was performed using an Agilent 1200 series liquid chromatograph comprised of a G1379B degasser, G1312A binary pump, G1367C automatic liquid sampler and F1315C diode array detector. The mobile phases were aqueous (A) formic acid (0.1%) and methanolic (B) formic acid (0.1%). 25 µl of the *Prochlorococcus*-derived sample was injected onto a ZORBAX SB-C18 column (Agilent; 3.5 µm 4.6x150 mm) at a flow of 1 ml/min (starting with 100% A, ramping to 80% B at 25 min, ramping to 100% B at 35 min and holding until 55 min, ramping to 0% B at 65 min and holding until 75 min). Full scan absorbance data were acquired from 210 to 800 nm with a 2.0 nm step and 4 nm slit width. Mass spectrometry was performed in-line using an Agilent 6130 (single quadrupole) mass spectrometer with an atmospheric electrospray ionization source. Source conditions were as follows: drying gas at 11.5 L/min, nebulizer at 60 psig, drying gas temperature at 300 ^{o}C, capillary voltages at + or - 4000 V. Acquisition ranges were from 100-2000 Da in the positive mode and used a fragmentor at 4.0, threshold at 150 and a step size of 0.1. Data was processed using the molecular profiling software MZmine 2 (Pluskal et al., 2010). Ions with a minimum signal intensity at least 5-fold greater than the maximum noise level were detected using a centroid mass detector. Chromatograms were then built from the raw data using the same minimum signal intensity, a retention time tolerance of +/-5 s, and a mass tolerance of +/-0.3 *m/z*.

BaySeq

For statistical comparisons of metatranscriptomic samples from treatment and control time points, each sequence within a sample was assigned to a single reference

gene in the NCBI-nr database based on BLASTX alignment bit score. When a single sequence aligned equally well to multiple potential reference genes, it was assigned to the reference gene that was most frequently identified in the dataset. Whole community reference gene hit counts were normalized to the total reads that matched the database for an individual sample. Reference gene abundances between samples were compared using baySeq, a method that uses an empirical Bayes approach to detect patterns of differential gene expression within a set of samples (Hardcastle and Kelly, 2010). BaySeq can perform pairwise sample comparisons, but is also capable of more complex comparisons to account for experimental designs involving multiple sample groups, such as the two treatments used here. We took advantage of the ability of baySeq to extract information from multiple sample groups, and simultaneously evaluated five different differential gene expression models to categorize the differential expression of reference genes at the whole community level for each time point individually. The first model (DE.1) examined the reference gene counts from the control microcosm relative to both treatments, to identify the differential expression of genes that were common to both treatments. The second model (DE. 2) identified only those reference genes that were significantly differentially expressed in the HMWDOM treatment relative to both the control and the ProDOM treatment. The third model (DE.3) identified only those reference genes that were significantly differentially expressed in the ProDOM treatment relative to both the control and the HMWDOM treatment. Models DE.2 and DE.3 were used to identify biological signals specific to the degradation of each DOM source. The fourth model, DE.all identified those reference

genes that were differentially expressed in the Control, HMWDOM, and ProDOM data and accounted for varying levels of gene expression within a single reference gene across all three conditions. Finally, the fifth model, Non-differentially expressed (NDE) assessed the probability of the expression of a reference gene being unaffected by the treatments. Bayseq estimates a posterior probability of each of the models that define patterns of differential or non-differential expression for each reference gene, such that the sum of all probabilities for each of the five models for the count data for a single reference gene equals one. To detect the significance of the affect of a single treatment or both treatments, the posterior probabilities of certain models could be summed. For example, a reference gene was considered differentially expressed in the HMWDOM treatment if the summed posterior probabilities from models DE.2 and DE.4 were greater than 0.9, because both of these models account for an affect specifically due to this treatment. Similarly, a reference gene was considered differentially expressed in the ProDOM treatment if the summed posterior probabilities from models DE.3 and DE.4 were greater than 0.9. If the posterior probabilities from models DE.1 and DE.4 were greater than 0.9, then a reference gene was considered differentially expressed in both treatments at a similar level. Additionally, differentially expressed reference genes were counted as enriched or underrepresented in a treatment based on their fold change between treatment and control. Differentially expressed reference genes from each of these five models provided a preliminary framework with which to understand similarities and differences that occurred in the treatments through time and helped guide and refine subsequent analyses at the organism level (particularly categorizing

pathways as central versus auxiliary). The data used to generate the plot in figure 2C was obtained by the following analysis: 1) Enumerate the number of differentially expressed reference genes enriched in a single treatment for each individual species name 2) Assign each species name and its differentially expressed reference gene counts to a taxonomic order.

Taxon-specific ortholog clustering

Pairwise reciprocal best BLAST hits between translated coding sequences of reference genomes within a single group were compiled to generate ortholog cluster assignments. For *Prochlorococcus*, the 13 genomes were: *P. marinus* str. AS9601; *P. marinus* str. MIT 9202; *P. marinus* str. MIT 9211; *P. marinus* str. MIT 9215; *P. marinus* str. MIT 9301; *P. marinus* str. MIT 9303; *P. marinus* str. MIT 9312; *P. marinus* str. MIT 9313; *P. marinus* str. MIT 9515; *P. marinus* str. NATL1A; *P. marinus* str. NATL2A; *P. marinus* subsp. marinus str. CCMP1375; *P. marinus* subsp. pastoris str. CCMP1986/MED4. Four Pelagibacter genomes were included in our analyses and these were: *P. Ubique* HTCC 7211, *P. Ubique* HTCC1062; *P. Ubique* HTCC1002; *alpha proteobacterium* HIMB114. Seven OM60 genomes were included: *gamma proteobacterium* HIMB55, *gamma proteobacterium* NOR5-3, *gamma proteobacterium* NOR51-B, *Congregibacter litoralis* KT71, *marine gamma proteobacterium* HTCC2080, *gamma proteobacterium* IMCC3088, *marine gamma proteobacterium* HTCC2148. Identification of shared genes in each of these taxon specific groups used an e-value cutoff of 10^{-5} and required 30% alignment identity over 80% of the longer sequence. Functional annotation of ortholog clusters used KEGG Genomes annotations where available (Ogata et al., 1999). Genomes from

these groups lacking curated annotations were analyzed using the KEGG automated annotation pipeline (KAAS) (Moriya et al., 2007). In some cases, metatranscriptomic sequences were mapped to reference genes that were not derived from sequenced genomes (i.e. environmental clones). Where possible, these references were assigned to ortholog clusters based on single-directional peptide BLAST (significance cutoffs as above). cDNA reads from our experiment with top BLASTx hits to a reference gene belonging to one of these three taxon bins were then mapped to their respective ortholog cluster (Dataset S1). For sequences matching equally well to multiple genes within the database (i.e. to multiple taxa), all matches were required to fall within the Cyanobacteria for assignment to *Prochlorococcus*, within the SAR11 cluster for *Pelagibacter* and within the OM60 clade itself for OM60 reads. Taxon-specific ortholog count files were used in baySeq in pairwise differential gene expression tests to identify those orthologs that were either enriched or under-represented in a single treatment relative to the control at each time point. For taxon-specific analyses, we opted to do pairwise comparisons between a single treatment and sample at each time point for organism specific bins and tease apart the differences and similarities between treatments by examining differentially expressed orthologs in central and auxiliary metabolic pathways as outlined in the results and discussion. The structure for this analysis pipeline was informed and guided by preliminary results from the whole community baySeq analysis, which indicated that many differentially expressed reference genes shared between both treatments were due to growth signals such as ribosomal proteins. The differential gene expression of individual KEGG annotated

orthologs was used to direct and support comparisons of taxon-specific pathway abundances between treatment and control cDNA samples (Figure 3, Datasets S2-S5). Changes in pathway abundances supported by DE KOs between treatment and control time points for *Prochlorococcus* and *Pelagibacter* were displayed in heatmaps (Figure 3) which were generated in R using the heatmap.2 function in gplots (Warnes et al., 2009) (http://hosho.ees.hokudai.ac.jp/~kubo/Rdoc/library/gplots/html/00Index.html).

Many DE orthologs from *Prochlorococcus* and *Pelagibacter* were from central metabolic pathways involved in growth, biosynthetic, or photosynthetic responses, providing information about the physiological state of the cell. To more efficiently examine the differential expression of orthologs involved in the degradation of specific DOM compounds, DE KOs involved in central metabolic pathways were filtered from the complete list of all DE orthologs detected from these organisms. The complete list of central metabolic pathways used to filter DE orthologs for each organism can be found in Supplementary file 2, along with the resulting list of auxiliary pathways. To eliminate redundancy, this list of central metabolic pathways also includes any pathway represented in the heatmaps in Figure 3, and often includes pathways that had no representation among the cDNA reads (but were included in that organism's complete list of pathways because they were present among DNA reads). DE orthologs from auxiliary pathways for *Prochlorococcus* are in tables S1-2 and *Pelagibacter* in tables S7-8. In the case of the OM60 clade, the majority of DE occurred in the final two time points, and all DE orthologs detected as enriched or underrepresented are displayed in Tables S9-S12.

References

Hardcastle, T.J., and Kelly, K.A. (2010) baySeq: empirical Bayesian methods for identifying differential expression in sequence count data. *BMC Bioinformatics* **11**: 422.

McCarren, J., Becker, J.W., Repeta, D.J., Shi, Y., Young, C.R., Malmstrom, R.R., et al. (2010) Microbial community transcriptomes reveal microbes and metabolic pathways associated with dissolved organic matter turnover in the sea. *Proc Natl Acad Sci U S A* **107**: 16420-16427.

Moore, L.R., Coe, A., Zinser, E.R., Saito, M.A., Sullivan, M.B., Lindell, D., et al. (2007) Culturing the marine cyanobacterium Prochlorococcus. *Limnol. Oceanogr. Methods* **5**: 353-362.

Moriya, Y., Itoh, M., Okuda, S., Yoshizawa, A.C., and Kanehisa, M. (2007) KAAS: an automatic genome annotation and pathway reconstruction server. *Nucleic Acids Res* **35**: W182-W185.

Ogata, H., Goto, S., Sato, K., Fujibuchi, W., Bono, H., and Kanehisa, M. (1999) KEGG: Kyoto encyclopedia of genes and genomes. *Nucleic acids research* **27**: 29-34.

Pluskal, T., Castillo, S., Villar-Briones, A., and Oresic, M. (2010) MZmine 2: modular framework for processing, visualizing, and analyzing mass spectrometry-based molecular profile data. *BMC Bioinformatics* **11**: 395.

Stewart, F.J., Ottesen, E.A., and DeLong, E.F. (2010) Development and quantitative analyses of a universal rRNA-subtraction protocol for microbial metatranscriptomics. *ISME J* **4**: 896-907.

Warnes, G.R., Bolker, B., and Lumley, T. (2009) gplots: Various R programming tools for plotting data. *R package version* **2**.

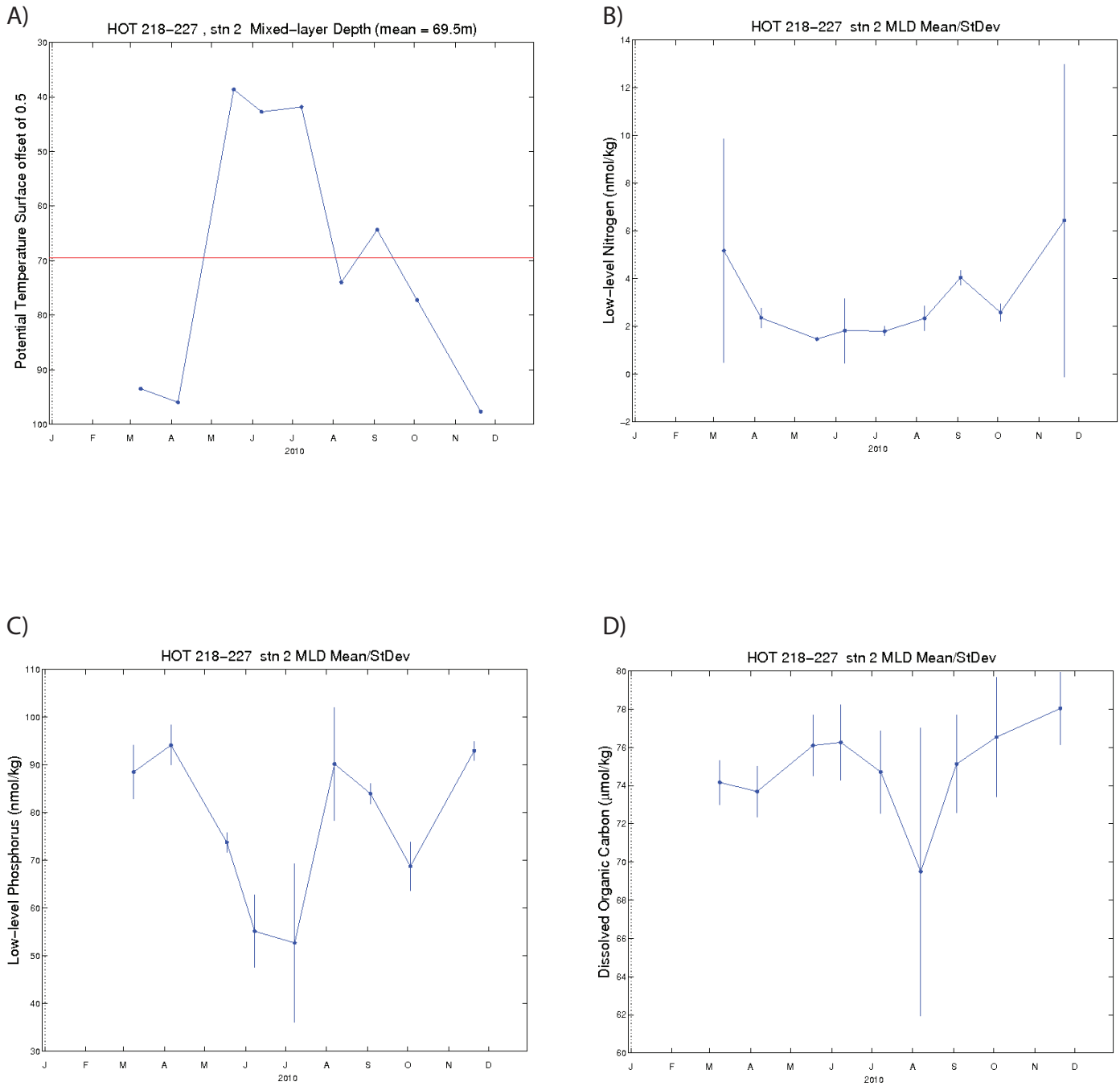

Supplementary Figure 1. Physiochemical characteristics of the mixed surface layer at Station ALOHA in 2010 plotted from the Hawaii Ocean Time-series Data Organization & Graphical System (HOT-DOGS) website (http://hahana.soest.hawaii.edu/hot/hot-dogs/) A) Monthly mixed layer depth calculated using potential temperature. B) Mean and standard deviation of monthly Low-level Nitrogen within the mixed layer depth. C) Mean and standard deviation of monthly Low-level Phosphate within the mixed layer depth. D) Mean and standard deviation of monthly Dissolved Organic Carbon within the mixed layer depth.

Table S1: Differentially expressed Prochlorococcus Orthologs enriched in HMWDOM belonging to auxiliary KEGG level 3 pathways[1]

Ortholog	KO	KEGG Level3[2]	Avg. fold change[3]	Time point[4]
Cluster 1909	K00540 K00273, DAO; D-amino-acid oxidase [EC:1.4.3.3]	00260 Glycine, serine and threonine metabolism 00472 D-Arginine and D-ornithine metabolism	7.96	2h (8:00 AM)
Cluster 729	K00812, aspB; aspartate aminotransferase [EC:2.6.1.1]	00250 Alanine, aspartate and glutamate metabolism 00330 Arginine and proline metabolism	3.76	2h (8:00 AM)
Cluster 172	K00297, metF; methylenetetrahydrofolate reductase (NADPH) [EC:1.5.1.20]	00680 Methane metabolism 00670 One carbon pool by folate	3.63	2h (8:00 AM)
Cluster 25	K00946, thiL; thiamine-monophosphate kinase [EC:2.7.4.16]	00730 Thiamine metabolism	3.04	2h (8:00 AM)
Cluster 1458	K00611, OTC, argF, argI; ornithine carbamoyltransferase [EC:2.1.3.3]	00330 Arginine and proline metabolism	2.41	2h (8:00 AM)
Cluster 53	K00620 argJ; glutamate N-acetyltransferase / amino-acid N-acetyltransferase [EC:2.3.1.35 2.3.1.1]	00330 Arginine and proline metabolism	3.98	12h (6:00 PM),36h (6:00 PM)
Cluster 449	K00286, proC; pyrroline-5-carboxylate reductase [EC:1.5.1.2]	00330 Arginine and proline metabolism	2.38	12h (6:00 PM),36h (6:00 PM)
Cluster 1180	K08479 sasA; two-component system, OmpR family, clock-associated histidine kinase SasA [EC:2.7.13.3]	02020 Two-component system 02022 Two-component system	5.70	27h (9:00 AM)
Cluster 2296	K03073 secE; preprotein translocase subunit SecE	02044 Secretion system 03060 Protein export	5.07	27h (9:00 AM)
Cluster 1344	rhomboid family membrane serine protease	01002 Peptidases	4.94	27h (9:00 AM)
Cluster 393	K01259 pip; proline iminopeptidase [EC:3.4.11.5]	00330 Arginine and proline metabolism 01002 Peptidases	4.65	27h (9:00 AM)
Cluster 1861	K01358 clpP, CLPP; ATP-dependent Clp protease, protease subunit [EC:3.4.21.92]	01002 Peptidases 04112 Cell cycle - Caulobacter	4.16	27h (9:00 AM)
Cluster 1490	putative signal peptidase; Signal peptidase I;	01002 Peptidases	2.94	27h (9:00 AM)
Cluster 227	ATP-dependent ClpB protease Hsp 100	01002 Peptidases	2.60	27h (9:00 AM),36h (6:00 PM)
Cluster 1812	K00820, K00820, glmS; glucosamine--fructose-6-phosphate aminotransferase (isomerizing) [EC:2.6.1.16]	00250 Alanine, aspartate and glutamate metabolism 00520 Amino sugar and nucleotide sugar	2.33	27h (9:00 AM),36h (6:00 PM)
Cluster 1858	K01714 dapA; dihydrodipicolinate synthase [EC:4.2.1.52]	00300 Lysine biosynthesis	1.73	27h (9:00 AM)
Cluster 147	K10697 rpaA; two-component system, OmpR family, response regulator RpaA	02020 Two-component system 02022 Two-component system	1.66	27h (9:00 AM)
Cluster 3062	K02473, wbpP; UDP-N-acetylglucosamine 4-epimerase [EC:5.1.3.7]	00520 Amino sugar and nucleotide sugar metabolism	inf	36h (6:00 PM)
Cluster 5393	K03116 tatA; sec-independent protein translocase protein TatA	03060 Protein export 03070 Bacterial secretion system	inf	36h (6:00 PM)
Cluster 1643	K00969 nadD; nicotinate-nucleotide adenylyltransferase [EC:2.7.7.18]	00760 Nicotinate and nicotinamide metabolism	10.53	36h (6:00 PM)
Cluster 623	K00383, GSR, gor; glutathione reductase (NADPH) [EC:1.8.1.7]	00480 Glutathione metabolism	5.26	36h (6:00 PM)
Cluster 339	K07738 nrdR; transcriptional repressor NrdR	03000 Transcription factors	2.98	36h (6:00 PM)
Cluster 1168	K01649, leuA; 2-isopropylmalate synthase [EC:2.3.3.13]	00290 Valine, leucine and isoleucine biosynthesis 00620 Pyruvate metabolism	2.87	36h (6:00 PM)

[1] Prochlorococcus orthologs detected among all cDNA and DNA samples in this experiment represented 140 KEGG level 3 pathways that were sorted into 50 core pathways and 90 auxiliary pathways. Core pathways were defined as those involved in DNA replication, cell growth, biosynthesis and photosynthesis. Auxiliary pathways represent the remainder of pathways. Only those Prochlorococcus orthologs that were detected as DE and belonged to an auxiliary KEGG level 3 pathway are represented. For each KO, only two pathways are shown. Sometimes a Prochlorococcus ortholog had two KO numbers, and in those cases, only a single functional annotation is represented. Peptiase orthologs without a KO number were manually assigned to a pathway based on NCBI annotation.

[2] Amino acid metabolism was included among the auxiliary pathways as it should be directly affected by increased nitrogen availability.

[3] Indicates the average fold change if the ortholog was differentially expressed at multiple time points

[4] Time point(s) that the ortholog was detected as differentially expressed

Table S2: Differentially expressed Prochlorococcus Orthologs enriched in ProDOM belonging to auxiliary KEGG level 3 pathways[1]

Ortholog	KO	KEGG Level3[2]	Avg. fold change[3]	Time point[4]
Cluster 1883	metal-dependent protease; conserved hypothetical protein ;	01002 Peptidases	inf	2h (8:00 AM)
Cluster 1909	K00540 K00273, DAO; D-amino-acid oxidase [EC:1.4.3.3]	00260 Glycine, serine and threonine metabolism 00472 D-Arginine and D-ornithine metabolism	9.35	2h (8:00 AM),12h (6:00 PM)
Cluster 5067	K01625 eda; 2-dehydro-3-deoxyphosphogluconate aldolase / 4-hydroxy-2-oxoglutarate aldolase [EC:4.1.2.14 4.1.3.16]	00030 Pentose phosphate pathway 00330 Arginine and proline metabolism	9.32	2h (8:00 AM)
Cluster 158	putative metal-dependent protease; putative molecular chaperone	01002 Peptidases	8.93	2h (8:00 AM)
Cluster 48	K01585, speA; arginine decarboxylase [EC:4.1.1.19]	00330 Arginine and proline metabolism	5.96	2h (8:00 AM)
Cluster 83	Dipeptidyl aminopeptidases/acylaminoacyl-peptidases	01002 Peptidases	4.86	2h (8:00 AM)
Cluster 623	K00383, GSR, gor; glutathione reductase (NADPH) [EC:1.8.1.7]	00480 Glutathione metabolism	4.40	2h (8:00 AM)
Cluster 25	K00946, thiL; thiamine-monophosphate kinase [EC:2.7.4.16]	00730 Thiamine metabolism	4.07	2h (8:00 AM)
Cluster 1528	K01255 CARP, pepA; leucyl aminopeptidase [EC:3.4.11.1]	01002 Peptidases 00480 Glutathione metabolism	3.07	2h (8:00 AM)
Cluster 1458	K00611, OTC, argF, argI; ornithine carbamoyltransferase [EC:2.1.3.3]	00330 Arginine and proline metabolism	2.79	2h (8:00 AM)
Cluster 172	K00297, metF; methylenetetrahydrofolate reductase (NADPH) [EC:1.5.1.20]	00680 Methane metabolism 00670 One carbon pool by folate	2.78	2h (8:00 AM)
Cluster 153	K11329 rpaB; two-component system, OmpR family, response regulator RpaB	02020 Two-component system 02022 Two-component system	1.77	2h (8:00 AM)
Cluster 1699	K10206, LL-diaminopimelate aminotransferase [EC:2.6.1.83]	00300 Lysine biosynthesis	1.77	2h (8:00 AM)
Cluster 1743	K03076 secY; preprotein translocase subunit SecY	03060 Protein export 03070 Bacterial secretion system	1.70	2h (8:00 AM)
Cluster 1344	rhomboid family membrane serine protease	01002 Peptidases	15.92	12h (6:00 PM),27h (9:00 AM)
Cluster 1848	K00794 ribH; riboflavin synthase beta chain [EC:2.5.1.-]	00740 Riboflavin metabolism	4.54	12h (6:00 PM)
Cluster 522	K03118 tatC; sec-independent protein translocase protein TatC	03060 Protein export 03070 Bacterial secretion system	3.92	12h (6:00 PM)
Cluster 1023	K03568 tldD; TldD protein	01002 Peptidases	3.53	12h (6:00 PM)
Cluster 1893	K00605, gcvT; aminomethyltransferase [EC:2.1.2.10]	00260 Glycine, serine and threonine metabolism 00910 Nitrogen metabolism	3.08	12h (6:00 PM)
Cluster 1812	K00820, glmS; glucosamine--fructose-6-phosphate aminotransferase (isomerizing) [EC:2.6.1.16]	00250 Alanine, aspartate and glutamate metabolism 00520 Amino sugar and nucleotide sugar	2.56	12h (6:00 PM)
Cluster 1830	K01077, phoA, phoB; alkaline phosphatase [EC:3.1.3.1]	00361 gamma-Hexachlorocyclohexane degradation 02020 Two-component system	2.37	12h (6:00 PM)
Cluster 504	K02259 COX15; cytochrome c oxidase subunit XV assembly protein	00860 Porphyrin and chlorophyll metabolism 00190 Oxidative phosphorylation	1.81	12h (6:00 PM)
Cluster 393	K01259 pip; proline iminopeptidase [EC:3.4.11.5]	00330 Arginine and proline metabolism 01002 Peptidases	4.06	27h (9:00 AM)
Cluster 1690	trypsin-like serine protease	01002 Peptidases	2.58	27h (9:00 AM)
Cluster 1508	K01358 clpP, CLPP; ATP-dependent Clp protease, protease subunit [EC:3.4.21.92]	01002 Peptidases 04112 Cell cycle - Caulobacter	2.22	27h (9:00 AM)
Cluster 1509	K01358 clpP, CLPP; ATP-dependent Clp protease, protease subunit [EC:3.4.21.92]	01002 Peptidases 04112 Cell cycle - Caulobacter	2.18	27h (9:00 AM)
Cluster 818	K00392, sir; sulfite reductase (ferredoxin) [EC:1.8.7.1]	00450 Selenoamino acid metabolism 00920 Sulfur metabolism	2.06	27h (9:00 AM)
Cluster 1643	K00969 nadD; nicotinate-nucleotide adenylyltransferase [EC:2.7.7.18]	00760 Nicotinate and nicotinamide metabolism	17.05	36h (6:00 PM)
Cluster 1187	K01583, K01582, lysine decarboxylase [EC:4.1.1.19]	00330 Arginine and proline metabolism 00310 Lysine degradation	5.07	36h (6:00 PM)
Cluster 449	K00286, proC; pyrroline-5-carboxylate reductase [EC:1.5.1.2]	00330 Arginine and proline metabolism	4.75	36h (6:00 PM)
Cluster 53	K00620 argJ; glutamate N-acetyltransferase / amino-acid N-acetyltransferase [EC:2.3.1.35 2.3.1.1]	00330 Arginine and proline metabolism	4.51	36h (6:00 PM)
Cluster 13	K01755, argH; argininosuccinate lyase [EC:4.3.2.1]	00250 Alanine, aspartate and glutamate metabolism 00330 Arginine and proline metabolism	4.03	36h (6:00 PM)
Cluster 339	K07738 nrdR; transcriptional repressor NrdR	03000 Transcription factors	3.34	36h (6:00 PM)
Cluster 36	K05912 K00436 E1.12.1.2; hydrogen dehydrogenase [EC:1.12.1.2]	00630 Glyoxylate and dicarboxylate metabolism 00680 Methane metabolism	2.12	36h (6:00 PM)
Cluster 350	K03797, prc, ctpA; carboxyl-terminal processing protease [EC:3.4.21.102]	01002 Peptidases	1.98	36h (6:00 PM)

[1] Prochlorococcus orthologsdetected among all cDNA and DNA samples in this experiment represented 140 KEGG level 3 pathways that were sorted into 50 core pathways and 90 auxiliary pathways. Core pathways were defined as those involved in DNA replication, cell growth, biosynthesis and photosynthesis. Auxiliary pathways represent the remainder of pathways. Only those Prochlorococcus orthologs that were detected as DE and belonged to an auxiliary KEGG level 3 pathway are represented. For each KO, only two pathways are shown. Sometimes a Prochlorococcus ortholog had two KO numbers, and in those cases, only a single functional annotation is represented. Peptiase orthologs without a KO number were manually assigned to a pathway based on NCBI annotation.

[2] Amino acid metabolism was included among the auxiliary pathways as it should be directly affected by increased nitrogen availability.

[3] Indicates the average fold change if the ortholog was differentially expressed at multiple time points

[4] Time point(s) that the ortholog was detected as differentially expressed

Table S3: Differentially expressed Pelagibacter transport Orthologs underrepresented in HMWDOM[1]

Ortholog	Annotation	Avg. fold change[2]	Time point[3]
Cluster 1009	K02029 ABC-type amino acid transport system, permease component	0.00	2h (8:00 AM)
Cluster 973	Probable ammonium transporter, marine subtype	0.43	2h (8:00 AM),12h (6:00 PM),27h (9:00 AM),36h (6:00 PM)
Cluster 643	K02002 Glycine betaine/proline transport system substrate-binding protein (proX)	0.44	2h (8:00 AM),12h (6:00 PM)
Cluster 600	K02051 Sulfonate/nitrate/taurine transport system substrate-binding protein (ssuA, tauA)	0.45	2h (8:00 AM)
Cluster 1323	K01999 Branched-chain amino acid transport system substrate-binding protein (livK)	0.57	2h (8:00 AM),12h (6:00 PM),27h (9:00 AM),36h (6:00 PM)
Cluster 1203	K09969 General L-amino acid transport system substrate-binding protein (aapJ, bztA)	0.59	2h (8:00 AM),12h (6:00 PM),27h (9:00 AM),36h (6:00 PM)
Cluster 971	TRAP-type bacterial extracellular solute-binding protein, family 7	0	12h (6:00 PM)
Cluster 1289	TRAP dicarboxylate transporter, dctp subunit	0.19	12h (6:00 PM)
Cluster 1830	TRAP-type extracellular solute-binding protein	0.22	12h (6:00 PM)
Cluster 753	K02002 Glycine betaine/proline transport system substrate-binding protein (proX)	0.30	12h (6:00 PM)
Cluster 2267	Ammonium transporter	0.36	12h (6:00 PM),27h (9:00 AM),36h (6:00 PM)
Cluster 1286	Ammonium transporter	0.50	12h (6:00 PM),36h (6:00 PM)
Cluster 1145	K06901 Xanthine/uracil/vitamin C permease family protein	0.53	12h (6:00 PM),27h (9:00 AM),36h (6:00 PM)
Cluster 688	K10018 Octopine/nopaline transport system substrate-binding protein (occT, nocT)	0.54	12h (6:00 PM)
Cluster 1786	K02027 ABC-type sugar transport system, periplasmic	0.55	12h (6:00 PM),36h (6:00 PM)
Cluster 297	TRAP dicarboxylate transporter - DctP subunit (mannitol/chloroaromatic compounds)	0.57	12h (6:00 PM)
Cluster 130	K01999 Branched-chain amino acid transport system substrate-binding protein (livK)	0.60	12h (6:00 PM),36h (6:00 PM)
Cluster 696	K02055 Spermidine/putrescine-binding periplasmic protein	0.70	12h (6:00 PM)
Cluster 1189	K02040 Phosphate transport system substrate-binding protein (pstS)	0.27	27h (9:00 AM)
Cluster 924	K02027 ABC-type sugar transport system, periplasmic	0.41	27h (9:00 AM),36h (6:00 PM)
Cluster 456	Arabinose efflux permease	0.42	27h (9:00 AM)
Cluster 557	K02195 Heme exporter protein C (ccmC)	0.44	36h (6:00 PM)
Cluster 462	TRAP-type bacterial extracellular solute-binding protein, family 7	0.58	36h (6:00 PM)

Table S4: Differentially expressed Pelagibacter transport Orthologs underrepresented in ProDOM[1]

Ortholog	Annotation	Avg. fold change[2]	Time point[3]
Cluster 971	bacterial extracellular solute-binding protein, family 7	0.04	2h (8:00 AM),12h (6:00 PM)
Cluster 1289	TRAP dicarboxylate transporter, dctp subunit	0.11	2h (8:00 AM)
Cluster 2267	Ammonium transporter	0.28	2h (8:00 AM),36h (6:00 PM)
Cluster 973	Probable ammonium transporter, marine subtype	0.40	2h (8:00 AM),12h (6:00 PM),36h (6:00 PM)
Cluster 1254	K02012 Iron(III) transport system substrate-binding protein (afuA, fbpA)	0.41	2h (8:00 AM)
Cluster 1286	Ammonium transporter	0.45	2h (8:00 AM),12h (6:00 PM)
Cluster 1145	K06901 Xanthine/uracil/vitamin C permease family protein	0.48	2h (8:00 AM),36h (6:00 PM)
Cluster 600	K02051 Sulfonate/nitrate/taurine transport system substrate-binding protein (ssuA, tauA)	0.48	2h (8:00 AM)
Cluster 1323	K01999 Branched-chain amino acid transport system substrate-binding protein (livK)	0.49	2h (8:00 AM),12h (6:00 PM)
Cluster 462	TRAP-type bacterial extracellular solute-binding protein, family 7	0.50	2h (8:00 AM),36h (6:00 PM)
Cluster 643	K02002 Glycine betaine/proline transport system substrate-binding protein (proX)	0.50	2h (8:00 AM),12h (6:00 PM)
Cluster 924	K02027 ABC-type sugar transport system, periplasmic	0.52	2h (8:00 AM)
Cluster 1203	K09969 General L-amino acid transport system substrate-binding protein (aapJ, bztA)	0.54	2h (8:00 AM),12h (6:00 PM)
Cluster 889	TRAP dicarboxylate transporter- dctp subunit	0.54	2h (8:00 AM)
Cluster 130	K01999 Branched-chain amino acid transport system substrate-binding protein (livK)	0.58	2h (8:00 AM),12h (6:00 PM),36h (6:00 PM)
Cluster 696	K02055 Spermidine/putrescine-binding periplasmic protein	0.68	2h (8:00 AM)
Cluster 1786	K02027 ABC-type sugar transport system, periplasmic	0.53	12h (6:00 PM)
Cluster 1189	K02040 Phosphate transport system substrate-binding protein (pstS)	0.23	27h (9:00 AM)

[1] DE Orthologs represented are either annotated with KEGG level 3 pathway 02000 Transporters or identified as transporters from ortholog annotations unassigned in KEGG

[2]Indicates the average fold change if the ortholog was differentially expressed at multiple time points

[3]Time point(s) that the ortholog was detected as differentially expressed

Table S5: Differentially expressed Pelagibacter transport Orthologs enriched in HMWDOM[1]

Ortholog	Annotation	Avg. fold change[2]	Time point[3]
Cluster 1389	K02196 Heme exporter protein D (ccmD)	inf	2h (8:00 AM)
Cluster 703	K02030 ABC-type amino acid transport substrate-binding protein (PheC)	2.54	2h (8:00 AM),36h (6:00 PM)
Cluster 3	K11720 Predicted permease YjgP/YjgQ family protein	inf	27h (9:00 AM)
Cluster 646	K02023 ABC sugar transporter, ATP-binding protein;	inf	27h (9:00 AM)
Cluster 1423	K07003 Resistance-Nodulation-Cell Division Superfamily transporter	2.47	27h (9:00 AM),36h (6:00 PM)
Cluster 698	K02010 Iron(III) transport system ATP-binding protein [EC:3.6.3.30]	14.19	36h (6:00 PM)
Cluster 865	K03499 Potassium transporter peripheral membrane componen (trka)	6.21	36h (6:00 PM)

Table S6: Differentially expressed Pelagibacter transport Orthologs enriched in ProDOM[1]

Ortholog	Annotation	Avg. fold change[2]	Time point[3]
Cluster 1389	K02196 Heme exporter protein D (ccmD)	inf	2h (8:00 AM)
Cluster 1492	K09013 FeS assembly ATPase SufC;	3.50	2h (8:00 AM)
Cluster 1423	K07003 Resistance-Nodulation-Cell Division Superfamily transporter	3.15	2h (8:00 AM)
Cluster 643	K02002 Glycine betaine/proline transport system substrate-binding protein (proX)	2.00	27h (9:00 AM)
Cluster 250	Lysine exporter protein; transporter;	3.92	36h (6:00 PM)
Cluster 703	K02030 ABC-type amino acid transport substrate-binding protein (PheC)	2.19	36h (6:00 PM)
Cluster 1203	K09969 General L-amino acid transport system substrate-binding protein (aapJ, bztA)	1.80	36h (6:00 PM)

[1] DE Orthologs represented are either annotated with KEGG level 3 pathway 02000 Transporters or identified as transporters from ortholog annotations unassigned in KEGG

[2]Indicates the average fold change if the ortholog was differentially expressed at multiple time points

[3]Time point(s) that the ortholog was detected as differentially expressed

Table S7: Differentially expressed Pelagibacter Orthologs enriched in HMWDOM belonging to auxiliary KEGG level 3 pathways[1]

Ortholog	KO	KEGG Level3[2]	Avg. fold change[3]	Time point[4]
Cluster 1393	K01586 lysA; diaminopimelate decarboxylase	00300 Lysine biosynthesis	6.13	12h (6:00 PM)
Cluster 577	K00013 hisD; histidinol dehydrogenase	00340 Histidine metabolism	5.82	12h (6:00 PM)
Cluster 647	K03072 secD; preprotein translocase subunit SecD	02044 Secretion system 03070 Bacterial secretion system	2.18	12h (6:00 PM)
Cluster 324	K03074 secF; preprotein translocase subunit SecF	02044 Secretion system 03070 Bacterial secretion system	2.90	12h (6:00 PM)
Cluster 896	K01755 argH, ASL; argininosuccinate lyase	00250 Alanine, aspartate and glutamate metabolism 00330 Arginine and proline metabolism	3.87	27h (9:00 AM)
Cluster 300	K01938 fhs; formate--tetrahydrofolate ligase	00630 Glyoxylate and dicarboxylate metabolism 00670 One carbon pool by folate	2.14	27h (9:00 AM)
Cluster 479	K07638 envZ; two-component system, OmpR family, osmolarity sensor histidine kinase EnvZ	02020 Two-component system	16.39	27h (9:00 AM)
Cluster 1220	K00820 E2.6.1.16, glmS; glucosamine--fructose-6-phosphate aminotransferase (isomerizing)	00250 Alanine, aspartate and glutamate metabolism 00520 Amino sugar and nucleotide sugar metabolism	6.88	2h (8:00 AM)
Cluster 14	K00240 sdhB; succinate dehydrogenase iron-sulfur protein	00020 Citrate cycle (TCA cycle) 00190 Oxidative phosphorylation	5.14	36h (6:00 PM)
Cluster 1279	K01653 E2.2.1.6S, ilvH, ilvN; acetolactate synthase I/III small subunit	00290 Valine, leucine and isoleucine biosynthesis 00650 Butanoate metabolism	inf	36h (6:00 PM)
Cluster 85	K00620 argJ; glutamate N-acetyltransferase / amino-acid N-acetyltransferase	00330 Arginine and proline metabolism	4.68	36h (6:00 PM)
Cluster 1084	K00075 murB; UDP-N-acetylmuramate dehydrogenase	00520 Amino sugar and nucleotide sugar metabolism 00550 Peptidoglycan biosynthesis	inf	36h (6:00 PM)
Cluster 612	K01069 E3.1.2.6, gloB; hydroxyacylglutathione hydrolase	00620 Pyruvate metabolism	inf	36h (6:00 PM)
Cluster 1363	K11175 purN; phosphoribosylglycinamide formyltransferase 1	00670 One carbon pool by folate 00230 Purine metabolism	inf	36h (6:00 PM)
Cluster 1587	K02221 yggt family protein	02044 Secretion system	11.35	36h (6:00 PM)
Cluster 1442	K02653 Type II Secretion System PilC;	02044 Secretion system 02035 Bacterial motility proteins	3.28	36h (6:00 PM)
Cluster 576	K03217 yidC, spoIIIJ, OXA1; preprotein translocase subunit YidC	02044 Secretion system 03070 Bacterial secretion system	2.26	36h (6:00 PM)

Table S8: Differentially expressed Pelagibacter Orthologs enriched in ProDOM belonging to auxiliary KEGG level 3 pathways[1]

Ortholog	KO	KEGG Level3[2]	Avg. fold change[3]	Time point[4]
Cluster 404	K01903 malate--CoA ligase subunit beta	00020 Citrate cycle (TCA cycle) 00640 Propanoate metabolism	10.96	2h (8:00 AM)
Cluster 85	K00620 argJ; glutamate N-acetyltransferase / amino-acid N-acetyltransferase	00330 Arginine and proline metabolism	7.09	2h (8:00 AM)
Cluster 752	K00641 E2.3.1.31, metX; homoserine O-acetyltransferase	00920 Sulfur metabolism 00270 Cysteine and methionine metabolism	3.03	2h (8:00 AM)
Cluster 1217	K01740 E2.5.1.49, metY; O-acetylhomoserine (thiol)-lyase	00270 Cysteine and methionine metabolism	2.52	2h (8:00 AM)
Cluster 837	K00471 E1.14.11.1; gamma-butyrobetaine dioxygenase	00310 Lysine degradation	4.09	12h (6:00 PM)
Cluster 1279	K01653 E2.2.1.6S, ilvH, ilvN; acetolactate synthase I/III small subunit	00290 Valine, leucine and isoleucine biosynthesis 00650 Butanoate metabolism	inf	36h (6:00 PM)
Cluster 664	K00858 E2.7.1.23; NAD+ kinase	00760 Nicotinate and nicotinamide metabolism	6.99	36h (6:00 PM)
Cluster 371	K04042 glmU; bifunctional UDP-N-acetylglucosamine pyrophosphorylase / Glucosamine-1-phosphate N-acetyltransferase	00520 Amino sugar and nucleotide sugar metabolism	4.78	36h (6:00 PM)
Cluster 450	K03210 yajC; preprotein translocase subunit YajC	02044 Secretion system 03070 Bacterial secretion system	3.19	36h (6:00 PM)

[1]*Pelagibacter* orthologs among all cDNA and DNA samples in this experiment represented 141 KEGG level 3 pathways that were sorted into 79 core pathways and 62 auxiliary pathways. Core pathways were defined as those generally involved in DNA replication, cell growth and biosynthetic processes. Auxiliary pathways represent non-core pathways. Only those Pelagibacter orthologs that were detected as DE and belonged to an auxiliary KEGG level 3 pathway are represented here. A single KO can sometimes belong to multiple pathways and in these instances only two pathways are shown. Sometimes a Pelagibacter ortholog had two KO numbers, and in those cases, only a single functional annotation is represented.

[2] Amino acid metabolism was included among the auxiliary pathways as it should be directly affected by increased nitrogen availability.

[3]Indicates the average fold change if the ortholog was differentially expressed at multiple time points

[4]Time point(s) that the ortholog was detected as differentially expressed

Table S9: Differentially expressed OM60 Orthologs enriched in HMWDOM[1]

Hierarchy	Annotation	KEGG Level3	Avg. fold change[2]	Time point[3]
Cluster 258	Cytochrome C' superfamily protein cytochrome c, class II protein cytochrome c556	unassigned	inf	2h (8:00 AM)
Cluster 277	K00939 E2.7.4.3, adk adenylate kinase (ATP-AMP transphosphorylase) [EC:2.7.4.3]	00230 Purine metabolism	inf	12h (6:00 PM)
Cluster 2332	K03551 ruvB holliday junction DNA helicase	03440 Homologous recombination 03400 DNA repair and recombination proteins	inf	27h (9:00 AM)
Cluster 3076	K00615 E2.2.1.1, tktA, tktB transketolase [EC:2.2.1.1]	00030 Pentose phosphate pathway 00710 Carbon fixation in photosynthetic organisms	inf	27h (9:00 AM)
Cluster 2148	K00820 E2.6.1.16, glmS glucosamine--fructose-6-phosphate aminotransferase (isomerizing) [EC:2.6.1.16]	00250 Alanine, aspartate and glutamate metabolism 00520 Amino sugar and nucleotide sugar metabolism	inf	27h (9:00 AM)
Cluster 2139	K02110 ATPF0C, atpE F-type H+-transporting ATPase subunit c [EC:3.6.3.14]	00190 Oxidative phosphorylation	inf	27h (9:00 AM)
Cluster 382	K00798 E2.5.1.17, cobO, btuR cob(I)alamin adenosyltransferase [EC:2.5.1.17]	00860 Porphyrin and chlorophyll metabolism	inf	27h (9:00 AM)
Cluster 1333	K02970 RP-S21, rpsU small subunit ribosomal protein S21	03011 Ribosome	inf	27h (9:00 AM), 36h (6:00 PM)
Cluster 4450	TonB-dependent receptor subfamily protein TonB-dependent receptor, plug	unassigned	inf	27h (9:00 AM), 36h (6:00 PM)
Cluster 9889	Glycosyl hydrolases family 16	unassigned	4.86	27h (9:00 AM)
Cluster 2112	K01878 glyQ glycyl-tRNA synthetase alpha chain [EC:6.1.1.14]	00970 Aminoacyl-tRNA biosynthesis	inf	36h (6:00 PM)
Cluster 8320	hypothetical protein MGP2080_01411	unassigned	inf	36h (6:00 PM)
Cluster 1937	K01887 RARS, argS arginyl-tRNA synthetase [EC:6.1.1.19]	00970 Aminoacyl-tRNA biosynthesis	inf	36h (6:00 PM)
Cluster 3300	K09903 pyrH Uridylate kinase UMP kinase [EC:2.7.4.22]	00240 Pyrimidine metabolism	12.04	36h (6:00 PM)
Cluster 1226	K03666 hfq RNA chaperone Hfq Host factor Hfq	03036 Chromosome 03018 RNA degradation	10.90	36h (6:00 PM)
Cluster 2758	K02916 RP-L35, rpmI large subunit ribosomal protein L35	03011 Ribosome	10.90	36h (6:00 PM)
Cluster 3107	K03561 transporter, MotA/TolQ/ExbB proton channel family protein TonB system biopolymer transport component	unassigned	3.31	36h (6:00 PM)

[1] Includes all OM60 orthologs detected as differentially expressed regardless of KEGG annotation

[2] Indicates the average fold change if the ortholog was differentially expressed at multiple time points

[3] Time point(s) that the ortholog was detected as differentially expressed

Table S10: Differentially expressed OM60 Orthologs enriched in ProDOM[1]

Hierarchy	Annotation	KEGG Level3	Avg. fold change[2]	Time point[3]
Cluster 268	K03317 putative Na+ dependent nucleoside transporter NupC protein	unassigned	inf	2h (8:00 AM)
Cluster 1965	K00324 pntA NAD(P) transhydrogenase subunit alpha [EC:1.6.1.2]	00760 Nicotinate and nicotinamide metabolism	inf	12h (6:00 PM)
Cluster 2133	K03495 tRNA uridine 5-carboxymethylaminomethyl modification enzyme GidA glucose-inhibited division protein A	03036 Chromosome	inf	12h (6:00 PM)
Cluster 1800	K06149 universal stress protein UspA-like protein universal stress protein family, putative	unassigned	inf	12h (6:00 PM)
Cluster 4573	K00099 dxr 1-deoxy-D-xylulose-5-phosphate reductoisomerase [EC:1.1.1.267]	00900 Terpenoid backbone biosynthesis	inf	12h (6:00 PM)
Cluster 5505	Predicted Fe-S oxidoreductase putative Fe-S oxidoreductase	unassigned	inf	12h (6:00 PM)
Cluster 1297	pentapeptide repeat domain protein	unassigned	inf	27h (9:00 AM)
Cluster 2148	K00820 E2.6.1.16, glmS glucosamine--fructose-6-phosphate aminotransferase (isomerizing) [EC:2.6.1.16]	00250 Alanine, aspartate and glutamate metabolism 00520 Amino sugar and nucleotide sugar metabolism	inf	27h (9:00 AM)
Cluster 2180	K01142 E3.1.11.2, xthA exodeoxyribonuclease III [EC:3.1.11.2]	03400 DNA repair and recombination proteins 03410 Base excision repair	inf	27h (9:00 AM)
Cluster 2539	K01689 ENO, eno enolase [EC:4.2.1.11] phosphopyruvate hydratase Enolase	00010 Glycolysis / Gluconeogenesis	inf	27h (9:00 AM)
Cluster 4450	TonB-dependent receptor subfamily protein TonB-dependent receptor, plug	unassigned	inf	27h (9:00 AM),36h (6:00 PM)
Cluster 3118	K00873 PK, pyk pyruvate kinase [EC:2.7.1.40] pyruvate kinase II	00620 Pyruvate metabolism 00010 Glycolysis / Gluconeogenesis	11.88	27h (9:00 AM)
Cluster 192	K00382 DLD, lpd, pdhD dihydrolipoamide dehydrogenase [EC:1.8.1.4]	00020 Citrate cycle (TCA cycle) 00620 Pyruvate metabolism	5.62	27h (9:00 AM)
Cluster 193	K00658 DLST, sucB 2-oxoglutarate dehydrogenase E2 component (dihydrolipoamide succinyltransferase) [EC:2.3.1.61]	00020 Citrate cycle (TCA cycle) 00310 Lysine degradation	4.86	27h (9:00 AM)
Cluster 4655	K00526 E1.17.4.1B, nrdB, nrdF ribonucleoside-diphosphate reductase beta chain [EC:1.17.4.1]	00240 Pyrimidine metabolism 00230 Purine metabolism	4.73	27h (9:00 AM)
Cluster 2298	K00525 E1.17.4.1A, nrdA, nrdE ribonucleoside-diphosphate reductase alpha chain [EC:1.17.4.1]	00240 Pyrimidine metabolism 00230 Purine metabolism	2.58	27h (9:00 AM)
Cluster 1333	K02970 RP-S21, rpsU small subunit ribosomal protein S21	03010 Ribosome 03011 Ribosome	inf	36h (6:00 PM)
Cluster 1042	hypothetical protein MGP2080_03820 conserved hypothetical protein FlgN protein	unassigned	inf	36h (6:00 PM)
Cluster 3589	K00031 IDH1, IDH2, icd isocitrate dehydrogenase [EC:1.1.1.42]	00020 Citrate cycle (TCA cycle)	inf	36h (6:00 PM)
Cluster 3636	K03106 SRP54, ffh signal recognition particle subunit SRP54 (TC 3.A.5.1.1)	03060 Protein export 03070 Bacterial secretion system	inf	36h (6:00 PM)
Cluster 1937	K01887 RARS, argS arginyl-tRNA synthetase [EC:6.1.1.19]	00970 Aminoacyl-tRNA biosynthesis	inf	36h (6:00 PM)
Cluster 2234	K03671 Thioredoxin	03110 Chaperones and folding catalysts	inf	36h (6:00 PM)
Cluster 1040	K02386 flgA flagella basal body P-ring formation protein	02040 Flagellar assembly 02035 Bacterial motility proteins	inf	36h (6:00 PM)
Cluster 1701	TonB-dependent outer membrane receptor	unassigned	inf	36h (6:00 PM)
Cluster 2112	K01878 glyQ glycyl-tRNA synthetase alpha chain [EC:6.1.1.14]	00970 Aminoacyl-tRNA biosynthesis	inf	36h (6:00 PM)
Cluster 190	K01902 sucD succinyl-CoA synthetase alpha subunit [EC:6.2.1.5]	00020 Citrate cycle (TCA cycle)	inf	36h (6:00 PM)
Cluster 3627	K01733 E4.2.3.1, thrC threonine synthase [EC:4.2.3.1] Threonine synthase	00260 Glycine, serine and threonine metabolism 00750 Vitamin B6 metabolism	inf	36h (6:00 PM)
Cluster 7065	K01130 E3.1.6.1, aslA arylsulfatase [EC:3.1.6.1] Sulfatase, secreted	00140 Steroid hormone biosynthesis 00600 Sphingolipid metabolism	inf	36h (6:00 PM)
Cluster 3167	penicillin-binding protein, beta-lactamase class C	unassigned	inf	36h (6:00 PM)
Cluster 766	K00919 ispE 4-diphosphocytidyl-2-C-methyl-D-erythritol kinase [EC:2.7.1.148]	00900 Terpenoid backbone biosynthesis	inf	36h (6:00 PM)
Cluster 1021	K10941 flrA sigma-54 specific transcriptional regulator, flagellar regulatory protein A	03000 Transcription factors	inf	36h (6:00 PM)
Cluster 2762	K04764 integration host factor, alpha subunit	03036 Chromosome 03032 DNA replication proteins	inf	36h (6:00 PM)
Cluster 7376	K03071 secB preprotein translocase subunit SecB Protein export cytoplasm chaperone protein	03070 Bacterial secretion system 03110 Chaperones and folding catalysts	15.43	36h (6:00 PM)
Cluster 3117	K03704 putative 'Cold-shock' DNA-binding domain protein protein CspE	03000 Transcription factors	10.29	36h (6:00 PM)
Cluster 1226	K03666 hfq RNA chaperone Hfq Host factor Hfq	03036 Chromosome 03018 RNA degradation	9.82	36h (6:00 PM)
Cluster 3465	K06142 hypothetical protein MGP2080_08019 Outer membrane protein (OmpH-like)	unassigned	5.14	36h (6:00 PM)
Cluster 1084	K02952 RP-S13, rpsM small subunit ribosomal protein S13	03010 Ribosome 03011 Ribosome	3.68	36h (6:00 PM)
Cluster 3107	K03561 transporter, MotA/TolQ/ExbB proton channel family protein TonB system biopolymer transport component	unassigned	3.36	36h (6:00 PM)

[1] Includes all OM60 orthologs detected as differentially expressed regardless of KEGG annotation

[2]Indicates the average fold change if the ortholog was differentially expressed at multiple time points

[3]Time point(s) that the ortholog was detected as differentially expressed

Table S11: Differentially expressed OM60 Orthologs underrepresented in HMWDOM[1]

Hierarchy	Annotation	KEGG Level3	Avg fold change[2]	Time point[3]
Cluster 1453	aerobic-type carbon monoxide dehydrogenase, large subunit CoxL/CutL-like protein	unassigned	0.00	2h (8:00 AM)
Cluster 2338	K03640 18K peptidoglycan-associated outer membrane lipoprotein, secreted OmpA/MotB	unassigned	0.00	12h (6:00 PM)
Cluster 6892	K09516 RETSAT all-trans-retinol 13,14-reductase [EC:1.3.99.23] FAD dependent oxidoreductase domain protein	00830 Retinol metabolism	0.24	12h (6:00 PM), 36h (6:00 PM)
Cluster 7809	TonB-dependent receptor	unassigned	0.00	27h (9:00 AM)
Cluster 9740	K02275 coxB cytochrome c oxidase subunit II [EC:1.9.3.1]	00190 Oxidative phosphorylation	0.00	27h (9:00 AM)
Cluster 8518	TonB-dependent receptor	unassigned	0.00	27h (9:00 AM)
Cluster 4025	K02014 TonB-dependent receptor domain protein outer membrane receptor protein	unassigned	0.23	27h (9:00 AM), 36h (6:00 PM)
Cluster 7577	putative hexachlorocyclohexane dehydrochlorinase 1	unassigned	0.00	36h (6:00 PM)
Cluster 3451	K01474 hyuB N-methylhydantoinase B/acetone carboxylase, alpha subunit [EC:3.5.2.14]	00330 Arginine and proline metabolism	0.00	36h (6:00 PM)
Cluster 387	TonB-dependent receptor plug domain protein	unassigned	0.00	36h (6:00 PM)
Cluster 8853	TonB-dependent receptor	unassigned	0.00	36h (6:00 PM)
Cluster 64	K13482 xdhB xanthine dehydrogenase large subunit [EC:1.17.1.4]	00230 Purine metabolism	0.00	36h (6:00 PM)
Cluster 2921	K13643 iron-sulfur cluster assembly transcription factor IscR transcriptional regulator'	03000 Transcription factors	0.06	36h (6:00 PM)
Cluster 3712	K03088 SIG3.2, rpoE RNA polymerase sigma-70 factor	03020 RNA polymerase	0.10	36h (6:00 PM)
Cluster 4700	hypothetical protein OMB55_00019360 hypothetical protein MGP2080_08414	unassigned	0.16	36h (6:00 PM)
Cluster 8788	TonB-dependent receptor	unassigned	0.18	36h (6:00 PM)
Cluster 7324	K16089 K02014 putative TonB-dependent receptor hypothetical protein NOR51B_2110 Outer membrane protein	unassigned	0.26	36h (6:00 PM)
Cluster 5367	hypothetical protein MGP2080_00560 hypothetical protein IMCC3088_1417	unassigned	0.26	36h (6:00 PM)
Cluster 3689	hypothetical protein OMB55_00014460 conserved hypothetical protein secreted protein	unassigned	0.42	36h (6:00 PM)
Cluster 3082	outer membrane cobalamin receptor protein TonB-dependent receptor domain protein	unassigned	0.43	36h (6:00 PM)

[1] Includes all OM60 orthologs detected as differentially expressed regardless of KEGG annotation

[2] Indicates the average fold change if the ortholog was differentially expressed at multiple time points

[3] Time point(s) that the ortholog was detected as differentially expressed

Table S12: Differentially expressed OM60 Orthologs underrepresented in ProDOM[1]

Hierarchy	Annotation	KEGG Level3	Avg. fold change[2]	Time point[3]
Cluster 7809	TonB-dependent receptor	unassigned	0.00	12h (6:00 PM)
Cluster 4882	K02404 GTP-binding signal recognition particle SRP54 flagellar biosynthetic protein FlhF	02035 Bacterial motility proteins	0.00	12h (6:00 PM)
Cluster 27	K03314 nhaB Na+:H+ antiporter	unassigned	0.00	12h (6:00 PM)
Cluster 3548	K01690 edd phosphogluconate dehydratase [EC:4.2.1.12] 6-phosphogluconate dehydratase	00030 Pentose phosphate pathway	0.00	12h (6:00 PM)
Cluster 4025	K02014 TonB-dependent receptor domain protein outer membrane receptor protein	unassigned	0.23	12h (6:00 PM),27h (9:00 AM),36h (6:00 PM)
Cluster 1229	K01448 N-acetylmuramoyl-L-alanine amidase domain protein AmiC	03036 Chromosome	0.00	27h (9:00 AM)
Cluster 3615	DNA integration/recombination/inversion protein phage integrase family	unassigned	0.00	27h (9:00 AM)
Cluster 8325	hypothetical protein MGP2080_01466	unassigned	0.06	27h (9:00 AM)
Cluster 6468	K02014 TonB-dependent receptor domain protein Outer membrane protein	unassigned	0.06	27h (9:00 AM)
Cluster 7992	K00257 E1.3.99.- [EC:1.3.99.-] Butyryl-CoA dehydrogenase	00281 Geraniol degradation 00624 1- and 2-Methylnaphthalene degradation	0.07	27h (9:00 AM)
Cluster 5678	K00174 korA 2-oxoglutarate ferredoxin oxidoreductase subunit alpha [EC:1.2.7.3]	00020 Citrate cycle (TCA cycle) 00720 Reductive carboxylate cycle (CO2 fixation)	0.10	27h (9:00 AM)
Cluster 1127	K03073 secE preprotein translocase subunit SecE (TC 3.A.5.1.1)	03060 Protein export 03070 Bacterial secretion system	0.12	27h (9:00 AM)
Cluster 4700	hypothetical protein OMB55_00019360 hypothetical protein MGP2080_08414	unassigned	0.12	27h (9:00 AM)
Cluster 392	K01637 E4.1.3.1, aceA isocitrate lyase [EC:4.1.3.1]	00630 Glyoxylate and dicarboxylate metabolism	0.22	27h (9:00 AM)
Cluster 2316	K02014 TonB-dependent receptor domain protein outer membrane receptor protein	unassigned	0.27	27h (9:00 AM)
Cluster 3801	hypothetical protein NOR51B_2319 TonB-dependent receptor, plug	unassigned	0.25	27h (9:00 AM),36h (6:00 PM)
Cluster 6892	K09516 RETSAT all-trans-retinol 13,14-reductase [EC:1.3.99.23] FAD dependent oxidoreductase domain protein	00830 Retinol metabolism	0.25	27h (9:00 AM),36h (6:00 PM)
Cluster 4041	K00134 GAPDH, gapA glyceraldehyde 3-phosphate dehydrogenase [EC:1.2.1.12]	00010 Glycolysis / Gluconeogenesis	0.00	36h (6:00 PM)
Cluster 1317	K00966 GMPP mannose-1-phosphate guanylyltransferase [EC:2.7.7.13]	00051 Fructose and mannose metabolism 00520 Amino sugar and nucleotide sugar metabolism	0.00	36h (6:00 PM)
Cluster 6134	conserved hypothetical protein	unassigned	0.04	36h (6:00 PM)
Cluster 2974	K03320 Ammonium Transporter Family subfamily protein	unassigned	0.06	36h (6:00 PM)
Cluster 2503	RND transporter, HAE1/HME family, permease protein	unassigned	0.17	36h (6:00 PM)
Cluster 8788	TonB-dependent receptor	unassigned	0.18	36h (6:00 PM)
Cluster 5367	hypothetical protein MGP2080_00560 hypothetical protein IMCC3088_1417	unassigned	0.18	36h (6:00 PM)
Cluster 3712	K03088 SIG3.2, rpoE RNA polymerase sigma-70 factor	03020 RNA polymerase	0.19	36h (6:00 PM)
Cluster 4786	glycine/D-amino acid oxidase, deaminating; putative monomeric sarcosine oxidase	unassigned	0.22	36h (6:00 PM)
Cluster 3689	hypothetical protein OMB55_00014460 conserved hypothetical protein secreted protein	unassigned	0.28	36h (6:00 PM)
Cluster 7264	TonB-dependent receptor domain protein hypothetical protein NOR51B_558	unassigned	0.32	36h (6:00 PM)
Cluster 930	K00257 E1.3.99.- [EC:1.3.99.-] Acyl-CoA dehydrogenase	00281 Geraniol degradation 00624 1- and 2-Methylnaphthalene degradation	0.33	36h (6:00 PM)
Cluster 1528	K15987 V-type H(+)-translocating pyrophosphatase pyrophosphate-energized proton pump	unassigned	0.35	36h (6:00 PM)
Cluster 3082	outer membrane cobalamin receptor protein TonB-dependent receptor domain protein	unassigned	0.41	36h (6:00 PM)
Cluster 3201	Oar-like outer membrane protein protein, OmpA family	unassigned	0.42	36h (6:00 PM)

[1] Includes all OM60 orthologs detected as differentially expressed regardless of KEGG annotation

[2] Indicates the average fold change if the ortholog was differentially expressed at multiple time points

[3] Time point(s) that the ortholog was detected as differentially expressed